CHAPTER 4

L3 APPROXIMATION OF THE CAPUTO DERIVATIVE AND ITS APPLICATION TO TIME-FRACTIONAL WAVE EQUATION

In this chapter, we discuss about the two novel approximation namely (L3 and ML3) of the Caputo fractional derivative of order $\alpha \in (1,2)$ on uniform grid points. This chapter is structured as follows: In Section 4.2, we gave the formulation of novel L3 approximation for the Caputo derivative of order $\alpha \in (1,2)$. In Section 4.2.1, we propose a new difference scheme to solve the TFWE. In section 4.3 we modify the L3 approximation and proposed ML3 approximation for the Caputo derivative of order $\alpha \in (1,2)$. The L3 approximation is tested on four examples in section 4.4 to show its effectiveness and accuracy. Section 4.4.1 deals with the numerical examples on TFWE and comparative studies with the existing schemes. Numerical stability of the TFWEs have also been verified here. Finally, the chapter is concluded in Section 4.5.

4.1 Introduction

Consider the one dimensional time fractional wave equation (TFWE) [69, 70]:

$$ {}_0^C\mathrm{D}_t^{\alpha}\mathfrak{U}(x,t) = \mathfrak{U}_{xx}(x,t) + \mathfrak{f}(x,t), \quad (x,t) \in \Omega = [0,L] \times [0,T], \tag{4.1} $$

with the initial conditions

$$ \mathfrak{U}(x,0) = \phi_1(x), \quad \mathfrak{U}_t(x,0) = \phi_2(x); \tag{4.2} $$

and boundary conditions.

$$ \mathfrak{U}(0,t) = \psi_1(x), \quad \mathfrak{U}(L,t) = \psi_2(x). \tag{4.3} $$

Here ${}_0^C\mathrm{D}_t^{\alpha}\mathfrak{U}(x,t)$ is the Caputo fractional derivative of order $1 < \alpha < 2$, and $(x,t) \in \Omega = [0,L] \times [0,T]$.

4.1.1 Purpose and contribution of this chapter

Motivated by the idea of Alikhanov's latest work [107], we aim to develop a novel L3 approximation for the Caputo derivative of order $\alpha \in (1,2)$ at time level t_k. Then we modify the L3 approximation by using Hermite interpolation as given in [114] and name it as ML3 approximation. The contributions of the chapter are described in the following points:

- In L3 approximation we have used Lagrange's cubic interpolation polynomial on uniform grid points $[(t_{j-2},\mathfrak{U}_{j-2}), (t_{j-1},\mathfrak{U}_{j-1}), (t_j,\mathfrak{U}_j), (t_{j+1},\mathfrak{U}_{j+1})]$ for $2 \leq j \leq k-1$ and quadratic interpolation in the first subinterval $[t_0,t_1]$.

- In modified L3 (ML3) approximation we have used the cubic Hermite interpolation in the interval $[\mathfrak{t}_0, \mathfrak{t}_2]$ by using $(\mathfrak{t}_0, \mathfrak{U}_0)$, $(\mathfrak{t}_1, \mathfrak{U}_1)$, $(\mathfrak{t}_2, \mathfrak{U}_2)$, $(\mathfrak{t}_0, \mathfrak{U}'_0)$. For $3 \leq j \leq \mathsf{k} - 1$, we have used the same Lagrange's cubic interpolation polynomial as discussed in above point. At the first time level, we again use the quadratic Hermite interpolation in the interval $[\mathfrak{t}_0, \mathfrak{t}_1]$ by using $(\mathfrak{t}_0, \mathfrak{U}_0)$, $(\mathfrak{t}_1, \mathfrak{U}_1)$, $(\mathfrak{t}_0, \mathfrak{U}'_0)$.

- The proposed L3 and ML3 approximation are tested on four different examples which gives high accurate results. The L3 approximation is observed to be highly accurate and of second order for all α whereas the ML3 approximation gives highly accurate as compared with L3 approximation for the first two example but almost give the same accuracy for polynomial of degree > 3.

- The advantage of both the approximation is that it can be directly used to solve TFPDE when $\alpha \in (1, 2)$ without using the method of order reduction.

- A difference scheme is provided for solving the TFWE using this approximation. Three numerical examples of the TFWEs are also provided to validate the accuracy of the proposed scheme.

- A comparative study of the numerical results by our proposed difference scheme with the existing schemes in [69], and [111] shows the effectiveness and accuracy of our scheme.

- Computationally, the difference scheme is observed to be of second order in space and time both.

To our knowledge, the proposed L3 and ML3 approximation and the difference scheme are new and have not been reported so far to solve any TFPDE. The scheme can also be implemented on other nonlinear TFPDEs and in higher dimensional problems.

4.2 Formulation of the novel L3 approximation of the Caputo derivative

Let $\{\mathfrak{t}_{\mathfrak{k}} = \mathfrak{k}\tau,\ \mathfrak{k} = 0, 1, 2, ..., N;\ T = \tau N\}$ be the number of grid point in time direction. and $\mathfrak{t}_{\mathfrak{k}+\frac{1}{2}} = (\mathfrak{t}_{\mathfrak{k}+1} + \mathfrak{t}_{\mathfrak{k}})/2$, $\Delta^2\mathfrak{U}_j = \mathfrak{U}_{j+2} - 2\mathfrak{U}_{j+1} + \mathfrak{U}_j$ and $\Delta^3\mathfrak{U}_j = \mathfrak{U}_{j+3} - 3\mathfrak{U}_{j+2} + 3\mathfrak{U}_{j+1} - \mathfrak{U}_j$. Suppose $\mathfrak{U}(\mathfrak{t}) \in C^3[t_{-1}, \mathfrak{t}_{\mathfrak{k}}]$, $\mathfrak{k} \geq 0$. The Caputo derivatives of order $\alpha \in (1, 2)$ at any point $\mathfrak{t}_{\mathfrak{k}}$ is defined as

$$ {}_0^C\mathrm{D}_{\mathfrak{t}}^{\alpha}\mathfrak{U}(\mathfrak{t})|_{\mathfrak{t}=\mathfrak{t}_{\mathfrak{k}}} = \frac{1}{\Gamma(2-\alpha)} \int_0^{\mathfrak{t}_{\mathfrak{k}}} \frac{\mathfrak{U}''(s)}{(\mathfrak{t}_{\mathfrak{k}} - s)^{\alpha-1}} ds, \tag{4.4} $$

$$ = \frac{1}{\Gamma(2-\alpha)} \sum_{j=1}^{\mathfrak{k}} \int_{\mathfrak{t}_{j-1}}^{\mathfrak{t}_j} \frac{\mathfrak{U}''(s)}{(\mathfrak{t}_{\mathfrak{k}} - s)^{\alpha-1}} ds. \tag{4.5} $$

The main idea behind this new approximation is to approximate the function $\mathfrak{U}(\mathfrak{t})$ is approximated by the quadratic interpolation polynomial in the first subinterval $[\mathfrak{t}_0, \mathfrak{t}_1]$ and then by cubic interpolation polynomial in the remaining subintervals $[\mathfrak{t}_{j-1}, \mathfrak{t}_j]$, $2 \leq j \leq \mathfrak{k}$. Let $\Pi_{2,j}$ be the quadratic interpolating polynomials of $\mathfrak{U}(\mathfrak{t})$ by using three points $(\mathfrak{t}_{j-2}, \mathfrak{U}_{j-2})$, $(\mathfrak{t}_{j-1}, \mathfrak{U}_{j-1})$, $(\mathfrak{t}_j, \mathfrak{U}_j)$. Taking the constraints of the results onto the sub-interval $[\mathfrak{t}_{j-1}, \mathfrak{t}_j]$, we get

$$ \Pi_{2,j}\mathfrak{U}(\mathfrak{t}) = \mathfrak{U}_{j-2}\frac{(\mathfrak{t} - \mathfrak{t}_{j-1})(\mathfrak{t} - \mathfrak{t}_j)}{2\tau^2} + \mathfrak{U}_{j-1}\frac{(\mathfrak{t} - \mathfrak{t}_{j-2})(\mathfrak{t}_j - \mathfrak{t})}{\tau^2} + \mathfrak{U}_j\frac{(\mathfrak{t} - \mathfrak{t}_{j-2})(\mathfrak{t} - \mathfrak{t}_{j-1})}{2\tau^2}, \tag{4.6} $$

and

$$ (\Pi_{2,j}\mathfrak{U}(\mathfrak{t}))'' = \frac{1}{\tau^2}\Delta^2\mathfrak{U}_{j-2}. \tag{4.7} $$

Let $\Pi_{3,j}$ be the cubic interpolating polynomials of $\mathfrak{U}(\mathfrak{t})$ by using four points $(\mathfrak{t}_{j-2}, \mathfrak{U}_{j-2})$, $(\mathfrak{t}_{j-1}, \mathfrak{U}_{j-1})$, $(\mathfrak{t}_j, \mathfrak{U}_j)$ and $(\mathfrak{t}_{j+1}, \mathfrak{U}_{j+1})$. Taking the constraints of the results onto the sub-interval $[\mathfrak{t}_j, \mathfrak{t}_{j+1}]$, we get

$$\begin{aligned}\Pi_{3,j}\mathfrak{U}(\mathfrak{t}) = \mathfrak{U}_{j-2}\frac{(\mathfrak{t}-\mathfrak{t}_{j-1})(\mathfrak{t}-\mathfrak{t}_j)(\mathfrak{t}_{j+1}-\mathfrak{t})}{6\tau^3} + \mathfrak{U}_{j-1}\frac{(\mathfrak{t}-\mathfrak{t}_{j-2})(\mathfrak{t}-\mathfrak{t}_j)(\mathfrak{t}-\mathfrak{t}_{j+1})}{2\tau^3} \\ + \mathfrak{U}_j\frac{(\mathfrak{t}-\mathfrak{t}_{j-2})(\mathfrak{t}-\mathfrak{t}_{j-1})(\mathfrak{t}_{j+1}-\mathfrak{t})}{2\tau^3} + \mathfrak{U}_{j+1}\frac{(\mathfrak{t}-\mathfrak{t}_{j-2})(\mathfrak{t}-\mathfrak{t}_{j-1})(\mathfrak{t}-\mathfrak{t}_j)}{6\tau^3},\end{aligned} \tag{4.8}$$

and

$$(\Pi_{3,j}\mathfrak{U}(\mathfrak{t}))'' = \frac{1}{\tau^2}\Delta^2\mathfrak{U}_{j-2} + \frac{1}{\tau^3}(\mathfrak{t}-\mathfrak{t}_{j-1})\Delta^3\mathfrak{U}_{j-2}. \tag{4.9}$$

The error in cubic interpolation is given by

$$\begin{aligned}\mathfrak{U}(\mathfrak{t}) - \Pi_{3,j}\mathfrak{U}(\mathfrak{t}) = \frac{1}{24}\mathfrak{U}''''(\eta_j)(\mathfrak{t}-\mathfrak{t}_{j-2})(\mathfrak{t}-\mathfrak{t}_{j-1})(\mathfrak{t}-\mathfrak{t}_j)(\mathfrak{t}-\mathfrak{t}_{j+1}), \\ \text{where } \mathfrak{t}\in[\mathfrak{t}_j,\mathfrak{t}_{j+1}],\ \eta_j\in(\mathfrak{t}_{j-2},\mathfrak{t}_{j+1}),\ 1\le j\le \mathsf{k}.\end{aligned} \tag{4.10}$$

$$\begin{aligned}(\mathfrak{U}(\mathfrak{t}) - \Pi_{3,j}\mathfrak{U}(\mathfrak{t}))'' &= \frac{1}{12}\mathfrak{U}''''(\eta_j)\Big[(\mathfrak{t}-\mathfrak{t}_{j-2})(\mathfrak{t}-\mathfrak{t}_{j-1}) + (\mathfrak{t}-\mathfrak{t}_{j-2})(\mathfrak{t}-\mathfrak{t}_j) + (\mathfrak{t}-\mathfrak{t}_{j-2})(\mathfrak{t}-\mathfrak{t}_{j+1}) \\ &\qquad + (\mathfrak{t}-\mathfrak{t}_{j-1})(\mathfrak{t}-\mathfrak{t}_j) + (\mathfrak{t}-\mathfrak{t}_{j-1})(\mathfrak{t}-\mathfrak{t}_{j+1}) + (\mathfrak{t}-\mathfrak{t}_j)(\mathfrak{t}-\mathfrak{t}_{j+1})\Big], \\ &= \frac{1}{12}\mathfrak{U}''''(\eta_j)\phi(t).\end{aligned} \tag{4.11}$$

where

$$\begin{aligned}\phi(t) =&\Big[(\mathfrak{t}-\mathfrak{t}_{j-2})(\mathfrak{t}-\mathfrak{t}_{j-1}) + (\mathfrak{t}-\mathfrak{t}_{j-2})(\mathfrak{t}-\mathfrak{t}_j) + (\mathfrak{t}-\mathfrak{t}_{j-2})(\mathfrak{t}-\mathfrak{t}_{j+1}) \\ &+ (\mathfrak{t}-\mathfrak{t}_{j-1})(\mathfrak{t}-\mathfrak{t}_j) + (\mathfrak{t}-\mathfrak{t}_{j-1})(\mathfrak{t}-\mathfrak{t}_{j+1}) + (\mathfrak{t}-\mathfrak{t}_j)(\mathfrak{t}-\mathfrak{t}_{j+1})\Big]\end{aligned} \tag{4.12}$$

Now, from the definition of Caputo derivative at first time level $\mathfrak{t}_1$ is

$$
\begin{aligned}
{}_0^C\mathrm{D}_{\mathfrak{t}}^{\alpha}\mathfrak{U}(\mathfrak{t})|_{\mathfrak{t}=\mathfrak{t}_1} &= \frac{1}{\Gamma(2-\alpha)}\int_{\mathfrak{t}_0}^{\mathfrak{t}_1}\frac{\mathfrak{U}''(s)}{(\mathfrak{t}_1-s)^{\alpha-1}}ds,\\
&\approx \frac{1}{\Gamma(2-\alpha)}\int_{\mathfrak{t}_0}^{\mathfrak{t}_1}\frac{(\Pi_{2,1}\mathfrak{U}(s))''}{(\mathfrak{t}_1-s)^{\alpha-1}}ds,\\
&= \frac{1}{\Gamma(2-\alpha)}\int_{\mathfrak{t}_0}^{\mathfrak{t}_1}(\mathfrak{t}_1-s)^{1-\alpha}\frac{1}{\tau^2}\Delta^2\mathfrak{U}_{-1}ds,\\
&= \frac{\tau^{-\alpha}}{\Gamma(3-\alpha)}\Delta^2\mathfrak{U}_{-1},
\end{aligned}
$$

Now, the numerical approximation of the Caputo derivative for the time level $\mathfrak{t}_{\mathsf{k}},\ \mathsf{k}\geq 2$ is given by

$$
\begin{aligned}
{}_0^C\mathrm{D}_{\mathfrak{t}}^{\alpha}\mathfrak{U}(\mathfrak{t})|_{\mathfrak{t}=\mathfrak{t}_{\mathsf{k}}} &= \frac{1}{\Gamma(2-\alpha)}\int_{\mathfrak{t}_0}^{\mathfrak{t}_{\mathsf{k}}}\frac{\mathfrak{U}''(s)}{(\mathfrak{t}_{\mathsf{k}}-s)^{\alpha-1}}ds,\\
&= \frac{1}{\Gamma(2-\alpha)}\left[\int_{\mathfrak{t}_0}^{\mathfrak{t}_2}\frac{\mathfrak{U}''(s)}{(\mathfrak{t}_{\mathsf{k}}-s)^{\alpha-1}}ds+\sum_{j=2}^{\mathsf{k}-1}\int_{\mathfrak{t}_j}^{\mathfrak{t}_{j+1}}\frac{\mathfrak{U}''(s)}{(\mathfrak{t}_{\mathsf{k}}-s)^{\alpha-1}}ds\right],\\
&\approx \frac{1}{\Gamma(2-\alpha)}\left[\int_{\mathfrak{t}_0}^{\mathfrak{t}_2}\frac{(\Pi_{3,1}\mathfrak{U}(s))''}{(\mathfrak{t}_{\mathsf{k}}-s)^{\alpha-1}}ds+\sum_{j=2}^{\mathsf{k}-1}\int_{\mathfrak{t}_j}^{\mathfrak{t}_{j+1}}\frac{(\Pi_{3,j}\mathfrak{U}(s))''}{(\mathfrak{t}_{\mathsf{k}}-s)^{\alpha-1}}ds\right],\\
&= \frac{1}{\Gamma(2-\alpha)}\left[\int_{\mathfrak{t}_0}^{\mathfrak{t}_2}(\mathfrak{t}_{\mathsf{k}}-s)^{1-\alpha}\left(\frac{\Delta^2\mathfrak{U}_{-1}}{\tau^2}+(s-\mathfrak{t}_0)\frac{\Delta^3\mathfrak{U}_{-1}}{\tau^3}\right)\right.\\
&\qquad\left.+\sum_{j=2}^{\mathsf{k}-1}\int_{\mathfrak{t}_j}^{\mathfrak{t}_{j+1}}(\mathfrak{t}_{\mathsf{k}}-s)^{1-\alpha}\left(\frac{\Delta^2\mathfrak{U}_{j-2}}{\tau^2}+(s-\mathfrak{t}_{j-1})\frac{\Delta^3\mathfrak{U}_{j-2}}{\tau^3}\right)ds\right],
\end{aligned}
$$

$$
\begin{aligned}
{}_0^C\mathrm{D}_t^{\alpha}\mathfrak{U}(t)|_{t=t_k} =& \frac{\tau^{-\alpha}}{\Gamma(3-\alpha)}\Bigg[\left(\mathfrak{a}_0^k+\mathfrak{a}_1^k\right)\Delta^2\mathfrak{U}_{-1}+\left(\mathfrak{b}_0^k+\mathfrak{b}_1^k-\mathfrak{a}_0^k\right)\Delta^3\mathfrak{U}_{-1}\Bigg] \\
&+\Bigg[\sum_{j=2}^{k-1}\left(\mathfrak{a}_j^k\Delta^2\mathfrak{U}_{j-2}+\mathfrak{b}_j^k\Delta^3\mathfrak{U}_{j-2}\right)\Bigg], \\
=& \frac{\tau^{-\alpha}}{\Gamma(3-\alpha)}\Bigg[\left(\mathfrak{a}_0^k+\mathfrak{a}_1^k\right)\Delta^2\mathfrak{U}_{-1}+\left(\mathfrak{b}_0^k+\mathfrak{b}_1^k-\mathfrak{a}_0^k\right)\left(\Delta^2\mathfrak{U}_0-\Delta^2\mathfrak{U}_{-1}\right) \\
&+\sum_{j=2}^{k-1}\left(\mathfrak{a}_j^k\Delta^2\mathfrak{U}_{j-2}+\mathfrak{b}_j^k(\Delta^2\mathfrak{U}_{j-1}-\Delta^2\mathfrak{U}_{j-2})\right)\Bigg], \\
=& \frac{\tau^{-\alpha}}{\Gamma(3-\alpha)}\Bigg[\left(2\mathfrak{a}_0^k+\mathfrak{a}_1^k-\mathfrak{b}_0^k-\mathfrak{b}_1^k\right)\Delta^2\mathfrak{U}_{-1}+\left(\mathfrak{b}_0^k+\mathfrak{b}_1^k-\mathfrak{a}_0^k\right)\Delta^2\mathfrak{U}_0 \\
&+\sum_{j=2}^{k-2}\left(\mathfrak{a}_{j+1}^k-\mathfrak{b}_{j+1}^k+\mathfrak{b}_j^k\right)\Delta^2\mathfrak{U}_{j-1}+(\mathfrak{a}_2^k-\mathfrak{b}_2^k)\Delta^2\mathfrak{U}_0+\mathfrak{b}_{k-1}^k\Delta^2\mathfrak{U}_{k-2}\Bigg], \\
=& \frac{\tau^{-\alpha}}{\Gamma(3-\alpha)}\Bigg[\left(2\mathfrak{a}_k^{(\alpha)}+\mathfrak{a}_{k-1}^{(\alpha)}-\mathfrak{b}_k^{(\alpha)}-\mathfrak{b}_{k-1}^{(\alpha)}\right)\Delta^2\mathfrak{U}_{-1}+\left(\mathfrak{b}_k^{(\alpha)}+\mathfrak{b}_{k-1}^{(\alpha)}-\mathfrak{a}_k^{(\alpha)}\right)\Delta^2\mathfrak{U}_0 \\
&+\sum_{j=2}^{k-2}\left(\mathfrak{a}_{k-j-1}^{(\alpha)}-\mathfrak{b}_{k-j-1}^{(\alpha)}+\mathfrak{b}_{k-j}^{(\alpha)}\right)\Delta^2\mathfrak{U}_{j-1}+(\mathfrak{a}_{k-2}^{(\alpha)}-\mathfrak{b}_{k-2}^{(\alpha)})\Delta^2\mathfrak{U}_0+\mathfrak{b}_1^{(\alpha)}\Delta^2\mathfrak{U}_{k-2}\Bigg], \\
=& \frac{\tau^{-\alpha}}{\Gamma(3-\alpha)}\sum_{j=0}^{k-1}\mathfrak{c}_{k-j-1}^{(k,\alpha)}\Delta^2\mathfrak{U}_{j-1} \equiv {}_0\mathbb{D}_t^{\alpha}\mathfrak{U}(t_k). \qquad (4.13)
\end{aligned}
$$

Eqn. (4.13) is the required L3 approximation for the Caputo derivative of order $\alpha \in (1,2)$. The coefficients $\mathfrak{a}_j^{(\alpha)}$, $\mathfrak{b}_j^{(\alpha)}$ and $\mathfrak{c}_j^{(k,\alpha)}$ is defined for $0 \le j \le k-1$ as,

$$\mathfrak{a}_j^{(\alpha)} = (j+1)^{2-\alpha} - j^{2-\alpha}, \qquad (4.14)$$

$$\mathfrak{b}_j^{(\alpha)} = \frac{1}{(3-\alpha)}\{(j+1)^{3-\alpha} - j^{3-\alpha}\} + (j+1)^{2-\alpha} - 2j^{2-\alpha}. \qquad (4.15)$$

For $k = 1$,

$$\mathfrak{c}_0^{(k,\alpha)} = 1,$$

for $\mathsf{k} = 2$,

$$\mathfrak{c}_j^{(\mathsf{k},\alpha)} = \begin{cases} -\mathfrak{a}_2^{(\alpha)} + \mathfrak{b}_1^{(\alpha)} + \mathfrak{b}_2^{(\alpha)}, & j = 0, \\ \mathfrak{a}_1^{(\alpha)} + 2\mathfrak{a}_2^{(\alpha)} - \mathfrak{b}_1^{(\alpha)} - \mathfrak{b}_2^{(\alpha)}, & j = 1, \end{cases} \tag{4.16}$$

for $\mathsf{k} = 3$,

$$\mathfrak{c}_j^{(\mathsf{k},\alpha)} = \begin{cases} \mathfrak{b}_1^{(\alpha)} & j = 0, \\ \mathfrak{a}_1^{(\alpha)} - \mathfrak{a}_3^{(\alpha)} - \mathfrak{b}_1^{(\alpha)} + \mathfrak{b}_2^{(\alpha)} + \mathfrak{b}_3^{(\alpha)}, & j = 1, \\ \mathfrak{a}_2^{(\alpha)} + 2\mathfrak{a}_3^{(\alpha)} - \mathfrak{b}_2^{(\alpha)} - \mathfrak{b}_3^{(\alpha)}, & j = 2, \end{cases} \tag{4.17}$$

for $\mathsf{k} \geq 4$,

$$\mathfrak{c}_j^{(\mathsf{k},\alpha)} = \begin{cases} \mathfrak{b}_1^{(\alpha)} & j = 0, \\ \mathfrak{a}_j^{(\alpha)} - \mathfrak{b}_j^{(\alpha)} + \mathfrak{b}_{j+1}^{(\alpha)} & 1 \leq j \leq \mathsf{k} - 3, \\ \mathfrak{a}_{\mathsf{k}-2}^{(\alpha)} - \mathfrak{a}_{\mathsf{k}}^{(\alpha)} - \mathfrak{b}_{\mathsf{k}-2}^{(\alpha)} + \mathfrak{b}_{\mathsf{k}-1}^{(\alpha)} + \mathfrak{b}_{\mathsf{k}}^{(\alpha)}, & j = \mathsf{k} - 2, \\ \mathfrak{a}_{\mathsf{k}-1}^{(\alpha)} + 2\mathfrak{a}_{\mathsf{k}}^{(\alpha)} - \mathfrak{b}_{\mathsf{k}-1}^{(\alpha)} - \mathfrak{b}_{\mathsf{k}}^{(\alpha)}, & j = \mathsf{k} - 1. \end{cases} \tag{4.18}$$

Now, the truncation error of the L3 approximation is given in the following theorem.

Theorem 4.2.1. For any $\alpha \in (1, 2)$ and let $\mathsf{k} \geq 2$ assume that $\mathfrak{U}(\mathfrak{t}) \in C^3[\mathfrak{t}_{-1}, \mathfrak{t}_{\mathsf{k}}]$, we have

$${}_0^C\mathrm{D}_{\mathfrak{t}}^{\alpha}\mathfrak{U}(\mathfrak{t})|_{\mathfrak{t}=\mathfrak{t}_{\mathsf{k}}} - {}_0\,\mathbb{D}_{\mathfrak{t}}^{\alpha}\mathfrak{U}(\mathfrak{t}_{\mathsf{k}}) = \mathcal{O}(\tau^2). \tag{4.19}$$

Proof. Let

$${}_0^C\mathrm{D}_{\mathfrak{t}}^{\alpha}\mathfrak{U}(\mathfrak{t})|_{\mathfrak{t}=\mathfrak{t}_{\mathsf{k}}} - {}_0\mathbb{D}_{\mathfrak{t}}^{\alpha}\mathfrak{U}(\mathfrak{t}_{\mathsf{k}}) = R_0^2 + R_2^{j+1}. \tag{4.20}$$

$$R_0^2 = \frac{1}{\Gamma(2-\alpha)} \int_{t_0}^{t_2} \frac{\mathfrak{U}''(s)}{(t_k - s)^{\alpha-1}} ds - \frac{1}{\Gamma(2-\alpha)} \int_{t_0}^{t_2} \frac{(\Pi_{3,1}(s))''}{(t_k - s)^{\alpha-1}} ds, \tag{4.21}$$

$$= \frac{1}{\Gamma(2-\alpha)} \int_{t_0}^{t_2} \frac{(\mathfrak{U}(s) - \Pi_{3,1}(s))''}{(t_k - s)^{\alpha-1}} ds,$$

$$= \frac{1}{\Gamma(2-\alpha)} \int_{t_0}^{t_2} (t_k - s)^{1-\alpha} \frac{1}{12} \mathfrak{U}''''(\eta_1)\phi(s) ds, \quad \text{using (4.11)}$$

$$\leq \frac{11\tau^2}{12} \frac{M_1}{\Gamma(2-\alpha)} \int_{t_0}^{t_2} (t_k - s)^{1-\alpha} ds. \tag{4.22}$$

Here, $M_1 = \max_{t_0 \leq \eta_1 \leq t_2} \mathfrak{U}''''(\eta_1)$. The maximum value of $\phi(s)$ in the interval $[t_0, t_2] = 11\tau^2$. Therefore

$$R_0^2 \leq \frac{11}{12} \frac{\tau^2 M_1}{\Gamma(3-\alpha)} [T^{2-\alpha} - (t_k - t_2)^{2-\alpha}]. \tag{4.23}$$

Now,

$$R_2^{j+1} = \frac{1}{\Gamma(2-\alpha)} \sum_{j=2}^{k-1} \int_{t_j}^{t_{j+1}} \frac{\mathfrak{U}''(s)}{(t_k - s)^{\alpha-1}} ds - \frac{1}{\Gamma(2-\alpha)} \sum_{j=2}^{k-1} \int_{t_j}^{t_{j+1}} \frac{(\Pi_{3,j}(s))''}{(t_k - s)^{\alpha-1}} ds, \tag{4.24}$$

$$= \frac{1}{\Gamma(2-\alpha)} \sum_{j=2}^{k-1} \int_{t_j}^{t_{j+1}} \frac{(\mathfrak{U}(s) - \Pi_{3,j}(s))''}{(t_k - s)^{\alpha-1}} ds,$$

$$= \frac{1}{\Gamma(2-\alpha)} \sum_{j=2}^{k-1} \int_{t_j}^{t_{j+1}} (t_k - s)^{1-\alpha} \frac{1}{12} \mathfrak{U}''''(\eta_j)\phi(s) ds, \quad \text{using (4.11)}$$

$$\leq \frac{11\tau^2}{12} \frac{1}{\Gamma(2-\alpha)} \sum_{j=2}^{k-1} \int_{t_j}^{t_{j+1}} M_j (t_k - s)^{1-\alpha} ds. \tag{4.25}$$

Here, $M_j = \max_{\mathfrak{t}_{j-2}\leq\eta_j\leq\mathfrak{t}_{j+1}} \mathfrak{U}''''(\eta_j)$. The maximum value of $\phi(s)$ in the interval $[\mathfrak{t}_{j-2}, \mathfrak{t}_{j+1}] = 11\tau^2$. Let $M = \max_{\mathfrak{t}_{-1}\leq\eta_j\leq\mathfrak{t}_{\mathsf{k}}} \mathfrak{U}''''(\eta_j)$, therefore

$$R_2^{j+1} \leq \frac{11}{12}\frac{\tau^2 M}{\Gamma(3-\alpha)}(\mathfrak{t}_{\mathsf{k}} - \mathfrak{t}_2)^{2-\alpha}. \tag{4.26}$$

Adding (4.23) and (4.26), we get,

$$\begin{aligned} R_0^2 + R_2^{j+1} &\leq \frac{11}{12}\frac{\tau^2 M}{\Gamma(3-\alpha)}[T^{2-\alpha} - (\mathfrak{t}_{\mathsf{k}} - \mathfrak{t}_2)^{2-\alpha}] + \frac{11}{12}\frac{\tau^2 M}{\Gamma(3-\alpha)}(\mathfrak{t}_{\mathsf{k}} - \mathfrak{t}_2)^{2-\alpha} \\ &\leq \frac{MT^{2-\alpha}}{\Gamma(3-\alpha)}\tau^2 = \mathcal{O}(\tau^2). \end{aligned} \tag{4.27}$$

□

4.2.1 Derivation of numerical scheme for TFWE

In this section, we design the numerical scheme for TFWE (4.1)-(4.3) by using the novel L3 approximation (4.13). Let us discretize the rectangular domain $\Omega = [0, L] \times [0, T]$ in unform mesh by taking $\{\mathrm{x}_i = i\mathsf{h},\ i = 0, 1, 2, ..., M;\ L = \mathsf{h}M\}$ and $\{\mathfrak{t}_{\mathsf{k}} = \mathsf{k}\tau,\ \mathsf{k} = 0, 1, 2, ..., N;\ T = \tau N\}$. Here, M and N are number of grid points in space and time direction, respectively. The TFWE at each spatial grid point x_i and time level $\mathfrak{t}_{\mathsf{k}}$ can be written as

$${}_0^C\mathrm{D}_{\mathfrak{t}}^{\alpha}\mathfrak{U}(\mathrm{x}_i, \mathfrak{t}_{\mathsf{k}}) = \frac{\partial^2\mathfrak{U}(\mathrm{x}_i, \mathfrak{t}_{\mathsf{k}})}{\partial\mathrm{x}^2} + \mathfrak{f}(\mathrm{x}_i, \mathfrak{t}_{\mathsf{k}}), \tag{4.28}$$

with initial conditions

$$\mathfrak{U}(\mathrm{x}_i, 0) = \phi_1(\mathrm{x}_i),\ \mathfrak{U}_{\mathfrak{t}}(\mathrm{x}_i, 0) = \phi_2(\mathrm{x}_i), \tag{4.29}$$

and boundary conditions

$$\mathfrak{U}(0,\mathfrak{t}_{\mathsf{k}})=\psi_1(\mathfrak{t}_{\mathsf{k}}),\ \mathfrak{U}(L,\mathfrak{t}_{\mathsf{k}})=\psi_2(\mathfrak{t}_{\mathsf{k}}). \tag{4.30}$$

Applying the L3 approximation for Caputo derivative at time $\mathfrak{t}_1$, and central difference scheme for discretizing the second order space derivative in (4.28), we have

$$\mathbb{D}_{\mathfrak{t}}^{\alpha}\mathfrak{U}(\mathrm{x}_i,\mathfrak{t}_1)=\frac{\partial^2\mathfrak{U}(\mathrm{x}_i,\mathfrak{t}_1)}{\partial\mathrm{x}^2}+\mathfrak{f}(\mathrm{x}_i,\mathfrak{t}_1), \tag{4.31}$$

$$\frac{\tau^{-\alpha}}{\Gamma(3-\alpha)}\left(\mathfrak{U}_i^1-2\mathfrak{U}_i^0+\mathfrak{U}_i^{-1}\right)=\frac{1}{\mathsf{h}^2}(\mathfrak{U}_{i+1}^1-2\mathfrak{U}_i^1+\mathfrak{U}_{i-1}^1)+\mathfrak{f}_i^1. \tag{4.32}$$

In order to calculate the value of $\mathfrak{U}_i^{-1}$, we use the initial condition $\mathfrak{U}_{\mathfrak{t}}(\mathrm{x}_i,0)=\phi_2(\mathrm{x}_i)$, i.e.

$$\frac{\mathfrak{U}_i^0-\mathfrak{U}_i^{-1}}{\tau}=\phi_2(\mathrm{x}_i), \tag{4.33}$$

$$\mathfrak{U}_i^{-1}=\mathfrak{U}_i^0-\tau\phi_2(\mathrm{x}_i). \tag{4.34}$$

Let $\mu=\dfrac{\tau^{-\alpha}}{\Gamma(3-\alpha)}$. Now, rearranging the terms, we get

$$-2\mathfrak{U}_i^0+\mathfrak{U}_i^{-1}-\frac{1}{d}\mathfrak{f}_i^1=\frac{1}{\mu\mathsf{h}^2}\mathfrak{U}_{i+1}^1-\left(\frac{2}{\mu\mathsf{h}^2}+1\right)\mathfrak{U}_i^1+\frac{1}{\mu\mathsf{h}^2}\mathfrak{U}_{i-1}^1. \tag{4.35}$$

The value of $\mathfrak{U}_0^1$ and $\mathfrak{U}_M^1$ is given by using boundary conditions, i.e. $\mathfrak{U}_0^1=\psi_1(\mathfrak{t}_1)$ and $\mathfrak{U}_M^1=\psi_2(\mathfrak{t}_{\mathsf{k}})$. Now, the fully discrete scheme for the TFWE at time level $\mathfrak{t}_{\mathsf{k}}$ for $\mathsf{k}\geq 2$ is

$$\mathbb{D}_{\mathfrak{t}}^{\alpha}\mathfrak{U}(\mathrm{x}_i,\mathfrak{t}_{\mathsf{k}})=\frac{\partial^2\mathfrak{U}(\mathrm{x}_i,\mathfrak{t}_{\mathsf{k}})}{\partial\mathrm{x}^2}+\mathfrak{f}(\mathrm{x}_i,\mathfrak{t}_{\mathsf{k}}), \tag{4.36}$$

$$\mu\left[\sum_{j=0}^{k-1}\mathfrak{c}_{k-j-1}^{(k,\alpha)}\Delta^2\mathfrak{U}_i^{j-1}\right]=\frac{1}{h^2}(\mathfrak{U}_{i+1}^k-2\mathfrak{U}_i^k+\mathfrak{U}_{i-1}^k)+\mathfrak{f}_i^k, \tag{4.37}$$

re-arranging the terms, we get,

$$\begin{aligned}\mathfrak{c}_{k-1}^{(k,\alpha)}\mathfrak{U}_i^{-1}+(\mathfrak{c}_{k-2}^{(k,\alpha)}-2\mathfrak{c}_{k-1}^{(k,\alpha)})\mathfrak{U}_i^0+\sum_{j=2}^{k-1}(\mathfrak{c}_{k-j+1}^{(k,\alpha)}-2\mathfrak{c}_{k-j}^{(k,\alpha)}+\mathfrak{c}_{k-j-1}^{(k,\alpha)})\mathfrak{U}_i^{j-1}+(\mathfrak{c}_1^{(k,\alpha)}-2\mathfrak{c}_0^{(k,\alpha)})\mathfrak{U}_i^{k-1}\\ =\frac{1}{\mu h^2}\mathfrak{U}_{i+1}^k-\left(\frac{2}{\mu h^2}+\mathfrak{c}_0^{(k,\alpha)}\right)\mathfrak{U}_i^k+\frac{1}{\mu h^2}\mathfrak{U}_{i-1}^k+\frac{1}{\mu}\mathfrak{f}_i^k.\end{aligned} \tag{4.38}$$

Let $\mathbb{U}^k=[\mathfrak{U}_1^k,\mathfrak{U}_2^k,\ldots,\mathfrak{U}_{N-1}^k]^T$ denotes the solution at time level k then the matrix form of the numerical scheme is given by

$$\begin{cases}\mathbb{A}_1\mathbb{U}^1 &= -2\mathbb{U}^0+\mathbb{U}^{-1}-\mathbb{F}^1+\mathbb{G}^1 \qquad\qquad \text{for } k=1,\\ \mathbb{A}_k\mathbb{U}^k &= \mathfrak{c}_{k-1}^{(k,\alpha)}\mathbb{U}^{-1}+(\mathfrak{c}_{k-2}^{(k,\alpha)}-2\mathfrak{c}_{k-1}^{(k,\alpha)})\mathbb{U}^0+\sum_{j=2}^{k-1}(\mathfrak{c}_{k-j+1}^{(k,\alpha)}-2\mathfrak{c}_{k-j}^{(k,\alpha)}+\mathfrak{c}_{k-j-1}^{(k,\alpha)})\mathbb{U}^{j-1}\cdot\\ &\quad +(\mathfrak{c}_1^{(k,\alpha)}-2\mathfrak{c}_0^{(k,\alpha)})\mathbb{U}^{k-1}-\mathbb{F}^k+\mathbb{G}^k \qquad \text{for } k\geq 2.\end{cases} \tag{4.39}$$

where, the matrix $\mathbb{A}_k,\ k=1,2,\ldots,(N-1)$ is of order $(N-1)$ and is denoted by

$$\mathbb{A}_k=tridiag\left[\frac{1}{\mu h^2},\ -\left(\frac{2}{\mu h^2}+\mathfrak{c}_0^{(k,\alpha)}\right),\ \frac{1}{\mu h^2}\right],\ \text{for } k\geq 1, \tag{4.40}$$

and the vector $\mathbb{F}^k=\frac{1}{\mu}[\mathfrak{f}_1^k,\mathfrak{f}_2^k,\ldots,\mathfrak{f}_{N-1}^k]^T$ and $\mathbb{G}^k=\left[-\frac{1}{\mu h^2}\mathfrak{U}_1^0,0,\ldots,0,-\frac{1}{\mu h^2}\mathfrak{U}_1^M\right]^T$.

Remark 4.2.1. We can calculate $\mathfrak{U}_i^{-1}$ by using central difference such as $\mathfrak{U}_i^{-1}=\mathfrak{U}_i^1-2\tau\phi_2(x_i)$ then (4.35) can be rewritten as

$$-2\mathfrak{U}_i^0-\frac{1}{d}\mathfrak{f}_i^1-2\tau\phi_2(x_i)=\frac{1}{\mu h^2}\mathfrak{U}_{i+1}^1-\left(\frac{2}{\mu h^2}+2\right)\mathfrak{U}_i^1+\frac{1}{\mu h^2}\mathfrak{U}_{i-1}^1. \tag{4.41}$$

Algorithm 4: To evaluate the numerical solution of TFWE (4.1)-(4.3)

Input: The rectangular domain $\Omega = [0, L] \times [0, T]$, M, h=L/M, N, $\tau = T/N$, initial conditions $\phi_1(x)$, $\phi_2(x)$, boundary conditions $\psi_1(x)$, $\psi_2(x)$ and $\alpha \in (1, 2)$.

Output: The discrete solutions at each grid point (x_i, t_k)

for Numerical solution of TFWE by the difference scheme **do**

Step-1.1 Divide the rectangular domain in uniform step size $x_i = ih,\ i = 0, 1, \ldots M$ and $t_k = k\tau\ k = 0, 1, \ldots N$.

Step-1.2 Apply L3 approximation (4.13) to discretize the Caputo derivative in time and central difference scheme for spatial derivatives term.

Step-1.3 In order to calculate the value $\mathfrak{U}_i^0$ and $\mathfrak{U}_i^{-1}$, we use the initial condition $\mathfrak{U}(x_i, 0) = \phi_1(x_i)$ and $\mathfrak{U}_t(x_i, 0) = \phi_2(x_i)$ respectively.

Step-1.4 Use the boundary conditions $\mathfrak{U}(0, t) = \psi_1(x_i)$ and $\mathfrak{U}(0, L) = \psi_1(x_i)$ to calculate the values of $\mathfrak{U}_0^k$ and $\mathfrak{U}_M^k$, respectively.

Step-1.5 The difference scheme for the numerical solution at first time level $\mathfrak{U}_i^1$ is given in (4.35).

Step-1.6 Use this solution $\mathfrak{U}_i^1$ to get the numerical solution $\mathfrak{U}_i^k$ at time level t_k for $k \geq 2$ by the difference scheme (4.38).

Step-1.7 Repeat Step 1.6 and use all the values of $\mathfrak{U}_i^k$ at each previous time levels till we get the discrete solution of TFWE at each discritised points (x_i, t_k).

end

4.3 Formulation of modified L3 (ML3) approximation of the Caputo derivatives

In this section, we will present modified L3 approximation called (ML3 approximation) by using cubic Hermite interpolation. The modification we do here is to approximate the function $\mathfrak{U}(\mathfrak{t})$ in the first subinterval $[\mathfrak{t}_0, \mathfrak{t}_1]$ by quadratic Hermite interpolation by using data $(\mathfrak{t}_0, \mathfrak{U}_0)$, $(\mathfrak{t}_1, \mathfrak{U}_1)$, $(\mathfrak{t}_0, \mathfrak{U}'_0)$. Let $H_2(t)$ denote the quadratic Hermite interpolation polynomial as

$$H_2(\mathfrak{t}) = \mathfrak{U}_0 + (\mathfrak{t} - \mathfrak{t}_0)\mathfrak{U}'(\mathfrak{t}_0) + \frac{(\mathfrak{t} - \mathfrak{t}_0)^2}{\tau}\left(\frac{\Delta\mathfrak{U}_0}{\tau} - \mathfrak{U}'_0\right). \tag{4.42}$$

Taking 2nd derivative we get

$$H''_2(\mathfrak{t}) = \frac{2}{\tau^2}\left(\Delta\mathfrak{U}_0 - \tau\mathfrak{U}'_0\right). \tag{4.43}$$

Now, we approximate the function $\mathfrak{U}(\mathfrak{t})$ in the subinterval $[\mathfrak{t}_0, \mathfrak{t}_2]$ by cubic Hermite interpolation by using data points $(\mathfrak{t}_0, \mathfrak{U}_0)$, $(\mathfrak{t}_1, \mathfrak{U}_1)$, $(\mathfrak{t}_2, \mathfrak{U}_2)$, $(\mathfrak{t}_0, \mathfrak{U}'_0)$,

$$H_3(\mathfrak{t}) = \mathfrak{U}_0 + (\mathfrak{t} - \mathfrak{t}_0)\mathfrak{U}'_0 + \frac{(\mathfrak{t} - \mathfrak{t}_0)^2}{\tau}\left(\frac{\Delta\mathfrak{U}_0}{\tau} - \mathfrak{U}'_0\right) + \frac{(\mathfrak{t} - \mathfrak{t}_0)^2(\mathfrak{t} - \mathfrak{t}_1)}{4\tau^2}\left[\frac{\Delta^2\mathfrak{U}_0}{\tau} - \left(\frac{\Delta\mathfrak{U}_0}{\tau} - \mathfrak{U}'_0\right)\right]. \tag{4.44}$$

Taking 2nd derivative we get

$$H''_3(\mathfrak{t}) = \frac{2}{\tau^2}\left(\Delta\mathfrak{U}_1 - \tau\mathfrak{U}'_0\right) + \frac{1}{2\tau^3}(3\mathfrak{t} - 2\mathfrak{t}_0 - \mathfrak{t}_1)\left(\Delta^2\mathfrak{U}_0 - 2\Delta\mathfrak{U}_0 + 2\tau\mathfrak{U}'_0\right). \tag{4.45}$$

For the subinterval $[\mathfrak{t}_j, \mathfrak{t}_{j+1}]$ when $j \geq 2$, we approximate the function by using the cubic Lagrange's interpolation polynomial as defined in (4.9) on the four points

$(\mathfrak{t}_{j-2}, \mathfrak{U}_{j-2})$, $(\mathfrak{t}_{j-1}, \mathfrak{U}_{j-1})$, $(\mathfrak{t}_j, \mathfrak{U}_j)$, $(\mathfrak{t}_{j+1}, \mathfrak{U}_{j+1})$.

$$(\Pi_{3,j}\mathfrak{U}(\mathfrak{t}))'' = \frac{1}{\tau^2}\Delta^2\mathfrak{U}_{j-2} + \frac{1}{\tau^3}(\mathfrak{t} - \mathfrak{t}_{j-1})\Delta^3\mathfrak{U}_{j-2}. \tag{4.46}$$

Now, the Caputo derivative at first time level $\mathfrak{t}_1$ is

$$\begin{aligned}
{}_0^C\mathrm{D}_{\mathfrak{t}}^{\alpha}\mathfrak{U}(\mathfrak{t})|_{\mathfrak{t}=\mathfrak{t}_1} &= \frac{1}{\Gamma(2-\alpha)}\int_{\mathfrak{t}_0}^{\mathfrak{t}_1}\frac{\mathfrak{U}''(s)}{(\mathfrak{t}_1 - s)^{\alpha-1}}ds,\\
&\approx \frac{1}{\Gamma(2-\alpha)}\int_{\mathfrak{t}_0}^{\mathfrak{t}_1}\frac{(H_2''(s))}{(\mathfrak{t}_1 - s)^{\alpha-1}}ds,\\
&= \frac{1}{\Gamma(2-\alpha)}\int_{\mathfrak{t}_0}^{\mathfrak{t}_1}(\mathfrak{t}_1 - s)^{1-\alpha}\frac{2}{\tau^2}\left(\Delta\mathfrak{U}_0 - \tau\mathfrak{U}_0'\right)ds,\\
&\approx \frac{2\tau^{-\alpha}}{\Gamma(3-\alpha)}\left(\Delta\mathfrak{U}_0 - \tau\mathfrak{U}_0'\right).
\end{aligned}$$

The Caputo derivative at second time level $\mathfrak{t}_2$ is

$$\begin{aligned}
{}_0^C\mathrm{D}_{\mathfrak{t}}^{\alpha}\mathfrak{U}(\mathfrak{t})|_{\mathfrak{t}=\mathfrak{t}_2} &= \frac{1}{\Gamma(2-\alpha)}\int_{\mathfrak{t}_0}^{\mathfrak{t}_2}\frac{\mathfrak{U}''(s)}{(\mathfrak{t}_2 - s)^{\alpha-1}}ds,\\
&\approx \frac{1}{\Gamma(2-\alpha)}\int_{\mathfrak{t}_0}^{\mathfrak{t}_2}\frac{(H_3''(s))}{(\mathfrak{t}_2 - s)^{\alpha-1}}ds,\\
&= \frac{1}{\Gamma(2-\alpha)}\int_{\mathfrak{t}_0}^{\mathfrak{t}_2}(\mathfrak{t}_2 - s)^{1-\alpha}\Bigg[\frac{2}{\tau^2}\left(\Delta\mathfrak{U}_0 - \tau\mathfrak{U}_0'\right)\\
&\qquad + \frac{1}{2\tau^3}(3\mathfrak{t} - 2\mathfrak{t}_0 - \mathfrak{t}_1)\left(\Delta^2\mathfrak{U}_0 - 2\Delta\mathfrak{U}_0 + 2\tau\mathfrak{U}_0'\right)\Bigg]ds,\\
&= \frac{\tau^{-\alpha}}{\Gamma(3-\alpha)}\left[2^{3-\alpha}\left(\Delta\mathfrak{U}_0 - \tau\mathfrak{U}_0'\right) + \frac{1}{2}\left(\frac{3.2^{3-\alpha}}{3-\alpha} - 2^{2-\alpha}\right)\left(\Delta^2\mathfrak{U}_0 - 2\Delta\mathfrak{U}_0 + 2\tau\mathfrak{U}_0'\right)\right].
\end{aligned} \tag{4.47}$$

The Caputo derivative for the time level $\mathfrak{t}_{\mathsf{k}},\ \mathsf{k} \geq 3$ is given by

$$
\begin{aligned}
{}_{0}^{C}\mathrm{D}_{\mathfrak{t}}^{\alpha}\mathfrak{U}(\mathfrak{t})|_{\mathfrak{t}=\mathfrak{t}_{\mathsf{k}}} &= \frac{1}{\Gamma(2-\alpha)} \int_{\mathfrak{t}_0}^{\mathfrak{t}_{\mathsf{k}}} \frac{\mathfrak{U}''(s)}{(\mathfrak{t}_{\mathsf{k}}-s)^{\alpha-1}} ds, \\
&= \frac{1}{\Gamma(2-\alpha)} \left[\int_{\mathfrak{t}_0}^{\mathfrak{t}_2} \frac{\mathfrak{U}''(s)}{(\mathfrak{t}_{\mathsf{k}}-s)^{\alpha-1}} ds + \sum_{j=2}^{\mathsf{k}-1} \int_{\mathfrak{t}_j}^{\mathfrak{t}_{j+1}} \frac{\mathfrak{U}''(s)}{(\mathfrak{t}_{\mathsf{k}}-s)^{\alpha-1}} ds \right], \\
&\approx \frac{1}{\Gamma(2-\alpha)} \left[\int_{\mathfrak{t}_0}^{\mathfrak{t}_2} \frac{(H_3''(s))}{(\mathfrak{t}_{\mathsf{k}}-s)^{\alpha-1}} ds + \sum_{j=2}^{\mathsf{k}-1} \int_{\mathfrak{t}_j}^{\mathfrak{t}_{j+1}} \frac{(\Pi_{3,j}(s))''}{(\mathfrak{t}_{\mathsf{k}}-s)^{\alpha-1}} ds \right], \\
&= \frac{1}{\Gamma(2-\alpha)} \left[\int_{\mathfrak{t}_0}^{\mathfrak{t}_2} (\mathfrak{t}_{\mathsf{k}}-s)^{1-\alpha} \left[\frac{2}{\tau^2} \left(\Delta\mathfrak{U}_1 - \tau\mathfrak{U}_0' \right) \right. \right. \\
&\qquad \left. + \frac{1}{2\tau^3} (3\mathfrak{t} - 2\mathfrak{t}_0 - \mathfrak{t}_1) \left(\Delta^2\mathfrak{U}_0 - 2\Delta\mathfrak{U}_0 + 2\tau\mathfrak{U}_0' \right) \right] \\
&\qquad \left. + \sum_{j=2}^{\mathsf{k}-1} \int_{\mathfrak{t}_j}^{\mathfrak{t}_{j+1}} (\mathfrak{t}_{\mathsf{k}}-s)^{1-\alpha} \left(\frac{\Delta^2\mathfrak{U}_{j-2}}{\tau^2} + (s-\mathfrak{t}_{j-1}) \frac{\Delta^3\mathfrak{U}_{j-2}}{\tau^3} \right) ds \right], \\
&= \frac{\tau^{-\alpha}}{\Gamma(3-\alpha)} \left[2 \left(\mathsf{k}^{2-\alpha} - (\mathsf{k}-2)^{2-\alpha} \right) \left(\Delta\mathfrak{U}_0 - \tau\mathfrak{U}_0' \right) \right. \\
&\quad + \frac{1}{2} \left(\frac{3}{3-\alpha} \left(\mathsf{k}^{3-\alpha} - (\mathsf{k}-2)^{3-\alpha} \right) - 5(\mathsf{k}-2)^{2-\alpha} - \mathsf{k}^{2-\alpha} \right) \left(\Delta^2\mathfrak{U}_0 - 2\Delta\mathfrak{U}_0 + 2\tau\mathfrak{U}_0' \right) \\
&\qquad \left. + \sum_{j=2}^{\mathsf{k}-1} \left(\mathfrak{a}_j^{\mathsf{k}} \Delta^2\mathfrak{U}_{j-2} + \mathfrak{b}_j^{\mathsf{k}} \Delta^3\mathfrak{U}_{j-2} \right) \right], \\
&= \frac{\tau^{-\alpha}}{\Gamma(3-\alpha)} \left[2 \left(\mathfrak{a}_0^{\mathsf{k}} + \mathfrak{a}_1^{\mathsf{k}} \right) \left(\Delta\mathfrak{U}_0 - \tau\mathfrak{U}_0' \right) \right. \\
&\qquad + \frac{1}{2} \left[3 \left(\mathfrak{b}_0^{\mathsf{k}} + \mathfrak{b}_1^{\mathsf{k}} \right) - 4\mathfrak{a}_0^{\mathsf{k}} - \mathfrak{a}_1^{\mathsf{k}} \right] \left(\Delta^2\mathfrak{U}_0 - 2\Delta\mathfrak{U}_0 + 2\tau\mathfrak{U}_0' \right) \\
&\qquad \left. + \sum_{j=2}^{\mathsf{k}-1} \left[\mathfrak{a}_j^{\mathsf{k}} \Delta^2\mathfrak{U}_{j-2} + \mathfrak{b}_j^{\mathsf{k}} (\Delta^2\mathfrak{U}_{j-1} - \Delta^2\mathfrak{U}_{j-2}) \right] \right],
\end{aligned}
$$

On re-arranging the terms we get

$$
\begin{aligned}
{}_0^C\mathrm{D}_t^{\alpha}\mathfrak{U}(t)|_{t=t_k} \approx \frac{\tau^{-\alpha}}{\Gamma(3-\alpha)}\Bigg[&3\left(2a_k^{(\alpha)}+a_{k-1}^{(\alpha)}-(b_k^{(\alpha)}+b_{k-1}^{(\alpha)})\right)(\Delta\mathfrak{U}_0-\tau\mathfrak{U}_0')\\
&+\frac{1}{2}\left(-4a_k^{(\alpha)}-a_{k-1}^{(\alpha)}+3(b_k^{(\alpha)}+b_{k-1}^{(\alpha)})\right)\Delta^2\mathfrak{U}_0+\sum_{j=1}^{k-1}e_{k-j-1}^{(k,\alpha)}\Delta^2\mathfrak{U}_{j-1}\Bigg].\\
=&\frac{\tau^{-\alpha}}{\Gamma(3-\alpha)}\left[\mathfrak{d}_k^{(k,\alpha)}(\Delta\mathfrak{U}_0-\tau\mathfrak{U}_0')+\bar{\mathfrak{d}}_k^{(k,\alpha)}\Delta^2\mathfrak{U}_0+\sum_{j=1}^{k-1}e_{k-j-1}^{(k,\alpha)}\Delta^2\mathfrak{U}_{j-1}\right].
\end{aligned}
\tag{4.48}
$$

$$
\equiv {}_0\tilde{\mathbb{D}}_t^{\alpha}\mathfrak{U}(t_k).
$$

Eq.(4.48) is Modified L3 approximation denoted by ${}_0\tilde{\mathbb{D}}_t^{\alpha}\mathfrak{U}(t_k)$. The coefficients $a_j^{(\alpha)}$, $b_j^{(\alpha)}$ are defined in (4.14) and (4.15). The coefficients $\mathfrak{d}_j^{(k,\alpha)}$ and $\bar{\mathfrak{d}}_j^{(k,\alpha)}$ is defined as

for $k=1$,

$$
\mathfrak{d}_1^{(k,\alpha)}=2,\quad \bar{\mathfrak{d}}_1^{(k,\alpha)}=0
$$

, for $k\geq 2$,

$$
\mathfrak{d}_j^{(k,\alpha)}=3\left(2a_k^{(\alpha)}+a_{k-1}^{(\alpha)}-(b_k^{(\alpha)}+b_{k-1}^{(\alpha)})\right), \tag{4.49}
$$

$$
\bar{\mathfrak{d}}_j^{(k,\alpha)}=\frac{1}{2}\left(-4a_k^{(\alpha)}-a_{k-1}^{(\alpha)}+3(b_k^{(\alpha)}+b_{k-1}^{(\alpha)})\right). \tag{4.50}
$$

The coefficients $e_j^{(k,\alpha)}$ are defined as

for $k=2$,

$$
e_0^{(k,\alpha)}=0,
$$

for $\mathsf{k} = 3$,

$$\mathfrak{e}_j^{(\mathsf{k},\alpha)} = \begin{cases} \mathfrak{b}_1^{(\alpha)}, & j = 0, \\ \mathfrak{a}_1^{(\alpha)} - \mathfrak{b}_1^{(\alpha)}, & j = 1, \end{cases} \tag{4.51}$$

for $\mathsf{k} \geq 4$,

$$\mathfrak{e}_j^{(\mathsf{k},\alpha)} = \begin{cases} \mathfrak{b}_1^{(\alpha)}, & j = 0, \\ \mathfrak{a}_j^{(\alpha)} - \mathfrak{b}_j^{(\alpha)} + \mathfrak{b}_{j+1}^{(\alpha)}, & 1 \leq j \leq \mathsf{k} - 3, \\ \mathfrak{a}_{\mathsf{k}-2}^{(\alpha)} - \mathfrak{b}_{\mathsf{k}-2}^{(\alpha)}, & j = \mathsf{k} - 2. \end{cases} \tag{4.52}$$

4.4 Numerical Examples

In this section, we apply the L3 and ML3 approximations on four numerical examples to demonstrate the effectiveness of the numerical schemes. Let $0 = \mathfrak{t}_0 < \mathfrak{t}_1 < \mathfrak{t}_2 < \cdots < \mathfrak{t}_N = T$ be the partition and $\tau = T/N$ is the time step size where $N = 10 \times 2^n$, $n = 0, 1, \ldots 6$. The computational error and order of convergence (CO) for $\alpha = 1.1, 1.5, 1.9$ at $\mathfrak{t}_N = 1$ is given in Table 4.1-4.4.

Example 4.4.1. Consider the function $\mathfrak{U}(\mathfrak{t}) = \mathfrak{t}^2$, then exact solution is given by

$${}_0^C\mathrm{D}_{\mathfrak{t}}^{\alpha}\mathfrak{U}(\mathfrak{t}) = \frac{2}{\Gamma(3-\alpha)}\mathfrak{t}^{2-\alpha}. \tag{4.53}$$

The maximum absolute error (MAE) and order of convergence (CO) is given below

Approx.	τ	α = 1.1		α = 1.5		α = 1.9	
		MAE	CO	MAE	CO	MAE	CO
L3	1/10	7.025E-04	0	2.213E-03	0	7.757E-04	0
	1/20	1.651E-04	2.089	5.083E-04	2.122	1.741E-04	2.156
	1/40	4.010E-05	2.042	1.221E-04	2.057	4.138E-05	2.073
	1/80	9.884E-06	2.020	2.995E-05	2.028	1.009E-05	2.035
	1/160	2.454E-06	2.010	7.416E-06	2.014	2.493E-06	2.017
	1/320	6.113E-07	2.005	1.845E-06	2.007	6.196E-07	2.009
	1/640	1.526E-07	2.002	4.602E-07	2.003	1.543E-07	2.006
ML3	1/10	4.441E-16	-	3.109E-15	-	2.087E-14	-
	1/20	3.109E-15	-2.807	2.398E-14	-2.948	1.239E-13	-2.570
	1/40	6.661E-15	-1.100	3.020E-14	-0.333	1.044E-13	0.248
	1/80	2.354E-14	-1.821	2.749E-13	-3.186	2.393E-12	-4.519
	1/160	7.994E-15	1.558	2.522E-13	0.124	3.656E-12	-0.611
	1/320	1.341E-13	-4.068	2.267E-12	-3.168	2.982E-11	-3.028
	1/640	1.257E-13	0.094	4.840E-12	-1.094	1.104E-10	-1.888

TABLE 4.1: The maximum absolute error (MAE) and order of convergence of example 4.4.1

Example 4.4.2. Consider the function $\mathfrak{U}(\mathfrak{t}) = \mathfrak{t}^3$, then the exact solution is given by

$$ {}_0^C\mathrm{D}_\mathfrak{t}^\alpha \mathfrak{U}(\mathfrak{t}) = \frac{6}{\Gamma(4-\alpha)}\mathfrak{t}^{3-\alpha}. \tag{4.54} $$

The maximum absolute error (MAE) and order of convergence is given below

Approx.	τ	$\alpha = 1.1$		$\alpha = 1.5$		$\alpha = 1.9$	
		MAE	CO	MAE	CO	MAE	CO
L3	1/10	4.641E-03	0	2.699E-03	0	4.820E-04	0
	1/20	1.165E-03	1.994	6.919E-04	1.964	1.268E-04	1.927
	1/40	2.919E-04	1.997	1.747E-04	1.985	3.232E-05	1.972
	1/80	7.305E-05	1.999	4.389E-05	1.993	8.148E-06	1.988
	1/160	1.827E-05	1.999	1.100E-05	1.997	2.045E-06	1.994
	1/320	4.568E-06	2.000	2.752E-06	1.998	5.122E-07	1.997
	1/640	1.142E-06	2.000	6.883E-07	1.999	1.280E-07	2.000
ML3	1/10	2.220E-15		1.776E-15		4.441E-15	
	1/20	7.994E-15	-1.848	5.862E-14	-5.044	2.851E-13	-6.005
	1/40	3.553E-15	1.170	7.105E-15	3.044	1.750E-13	0.704
	1/80	3.242E-14	-3.190	3.570E-13	-5.651	2.911E-12	-4.056
	1/160	5.773E-15	2.489	3.038E-13	0.233	4.733E-12	-0.701
	1/320	2.331E-13	-5.336	3.947E-12	-3.700	5.240E-11	-3.469
	1/640	8.660E-14	1.429	1.369E-12	1.528	6.357E-11	-0.279

TABLE 4.2: The maximum absolute error (MAE) and order of convergence of example 4.4.2

.

Remark 4.4.1. From Table 4.1 and 4.2 we can see that ML3 approximation (4.48) gives higher accuracte result than L3 approximation (4.13) but the order of convergence not second order in case of polynomial of degree 2 and 3.

Example 4.4.3. Consider the function $\mathfrak{U}(\mathfrak{t}) = \mathfrak{t}^4$, then,

$$ {}_0^C\mathrm{D}_\mathfrak{t}^\alpha \mathfrak{U}(\mathfrak{t}) = \frac{24}{\Gamma(5-\alpha)} \mathfrak{t}^{4-\alpha}. \tag{4.55} $$

The maximum absolute error (MAE) and order of convergence is given below

Approx.	τ	α = 1.1		α = 1.5		α = 1.9	
		MAE	CO	MAE	CO	MAE	CO
L3	1/10	7.323E-02	0	1.014E-01	0	1.785E-01	0
	1/20	1.959E-02	1.903	2.497E-02	2.021	4.322E-02	2.046
	1/40	5.052E-03	1.955	6.119E-03	2.029	1.046E-02	2.048
	1/80	1.282E-03	1.979	1.501E-03	2.027	2.529E-03	2.047
	1/160	3.228E-04	1.990	3.695E-04	2.023	6.123E-04	2.046
	1/320	8.097E-05	1.995	9.124E-05	2.018	1.484E-04	2.045
	1/640	2.028E-05	1.998	2.260E-05	2.014	3.599E-05	2.044
ML3	1/10	7.319E-02		1.013E-01		1.785E-01	
	1/20	1.958E-02	1.902	2.496E-02	2.028	4.322E-02	2.046
	1/40	5.052E-03	1.955	6.119E-03	2.028	1.046E-02	2.047
	1/80	1.282E-03	1.979	1.501E-03	2.027	2.529E-03	2.047
	1/160	3.228E-04	1.990	3.695E-04	2.023	6.123E-04	2.046
	1/320	8.097E-05	1.998	9.124E-05	2.018	1.484E-04	2.045
	1/640	2.028E-05	1.998	2.260E-05	2.014	3.559E-05	2.044

TABLE 4.3: The maximum absolute error (MAE) and order of convergence of example 4.4.3

Example 4.4.4. Let $\mathfrak{U}(\mathfrak{t}) = \mathfrak{t}^{2+\alpha}$, then we have

$$ {}_0^C\mathrm{D}_\mathfrak{t}^\alpha \mathfrak{U}(\mathfrak{t}) = \frac{\Gamma(3+\alpha)}{2}\mathfrak{t}^2. \tag{4.56} $$

The maximum absolute error (MAE) and order of convergence is given below

Approx.	τ	α = 1.1		α = 1.5		α = 1.9	
		MAE	CO	MAE	CO	MAE	CO
L3	1/10	5.696E-03	0	3.760E-02	0	1.464E-01	0
	1/20	1.712E-03	1.735	9.478E-03	1.988	3.527E-02	2.054
	1/40	4.945E-04	1.791	2.385E-03	1.991	8.513E-03	2.051
	1/80	1.391E-04	1.830	5.989E-04	1.993	2.058E-03	2.049
	1/160	3.839E-05	1.858	1.502E-04	1.995	4.980E-04	2.047
	1/320	1.044E-05	1.879	3.765E-05	1.997	1.207E-04	2.045
	1/640	2.806E-06	1.895	9.428E-06	1.998	2.928E-05	2.043
ML3	1/10	5.625E-03		3.742E-02		1.464E-01	
	1/20	1.704E-03	1.723	9.462E-03	1.983	3.527E-02	2.053
	1/40	4.936E-04	1.787	2.383E-03	1.989	8.513E-03	2.051
	1/80	1.390E-04	1.828	5.988E-04	1.993	2.058E-03	2.049
	1/160	3.838E-05	1.857	1.502E-04	1.995	4.980E-04	2.047
	1/320	1.044E-05	1.878	3.765E-05	1.997	1.207E-04	2.045
	1/640	2.806E-06	1.895	9.427E-06	1.998	2.928E-05	2.043

TABLE 4.4: The maximum absolute error (MAE) and order of convergence of example 4.4.4

Remark 4.4.2. From tables 4.3 and 4.4 we can see that both L3 and ML3 approximation gives same accuracy and order of convergence in case of polynomial of degree greater than 3.

4.4.1 Application to TFWEs

In this section, we have used the difference scheme (4.39) to solve the three different TFWE problems.

4.4.1.1 Numerical Stability

We have verified the stability of our scheme numerically by adding some disturbance (noise) in the initial data [166, 173]. Let $\mathfrak{U}^{\delta}(\mathrm{x},0)$ denotes the initial condition with the noise δ i.e.

$$\mathfrak{U}^{\delta}(\mathrm{x}_i,0)=\mathfrak{U}(\mathrm{x}_i,0)+\delta\omega, \tag{4.57}$$

where, ω is the uniform random variable whose values lies in $[-1,1]$, such that

$$\max_{1\leq i\leq\mathcal{M}}(\mathfrak{U}(\mathrm{x}_i,0)-\mathfrak{U}^{\delta}(\mathrm{x}_i,0))\leq\delta, \tag{4.58}$$

in our examples, we choose the noise δ=Maximum Absolute Error and $\mathcal{M}$=100 grid points.

Example 4.4.5. Consider the following TFWE with homogeneous boundary conditions

$${}_0^C\mathrm{D}_{\mathfrak{t}}^{\alpha}\mathfrak{U}(\mathrm{x},\mathfrak{t})=\frac{\partial^2\mathfrak{U}(\mathrm{x},\mathfrak{t})}{\partial\mathrm{x}^2}+\mathfrak{f}(\mathrm{x},\mathfrak{t}),\quad(\mathrm{x},\mathfrak{t})\in[0,1]\times[0,1] \tag{4.59}$$

with initial and boundary conditions

$$\mathfrak{U}(\mathrm{x},0)=0,\ \mathfrak{U}_{\mathfrak{t}}(\mathrm{x},0)=0,\quad 0\leq\mathrm{x}\leq 1, \tag{4.60}$$

$$\mathfrak{U}(0,\mathfrak{t})=0,\ \mathfrak{U}(1,\mathfrak{t})=0, \tag{4.61}$$

and source term

$$\mathfrak{f}(\mathrm{x},\mathfrak{t})=\left(\frac{6\mathfrak{t}^{3-\alpha}}{\Gamma(4-\alpha)}+\pi^2\mathfrak{t}^3\right)\sin(\pi\mathrm{x}). \tag{4.62}$$

The exact solution of Ex. 4.4.5 is given by [69],

$$\mathfrak{U}(x,t) = t^3 \sin(\pi x). \tag{4.63}$$

The following outcomes of Ex. 4.4.5 are:

- Fig. 4.1 and 4.2 shows absolute errors in Ex. 4.4.5, for $\alpha = 1.5$ and $\alpha = 1.9$ respectively, when $\tau = 1/100$ and $h = 1/100$. It shows that, at each time level the approximate solutions by using Algorithm 4 are in good agreement with the exact solution.

- Fig. 4.3 shows the absolute error at $T = 1$ for different value of α, when $\tau = 0.01$ and $h = 0.01$.

- The L_2 error and L_∞-error along with temporal order of convergence for $\alpha = 1.1, 1.5, 1.9$, at time $T = 1$ are provided in Table 4.5-4.6. We have taken $N = 40 \times 2^n$, $n = 0, 1, \ldots, 4$ and $M = 2000$ grid points.

- The L_2 error and L_∞ error along with spatial order of convergence for $\alpha = 1.1, 1.5, 1.9$, at time $T = 1$ are provided in Table 4.7-4.8 by taking We have taken $M = 5 \times 2^n$, $n = 0, 1, \ldots, 6$ and $N = 1000$ grid points. Therefore, we can conclude that the order of convergence of the numerical scheme is $\mathcal{O}(\tau^2, h^2)$ for all α.

- A comparative study of the L_2 and L_∞-error by the proposed scheme with the existing numerical results [69] are also provided in Table 4.9 for $\alpha = 1.1, 1.5, 1.9$ at time $T = 1$ by taking $h = 1/1000$. It can be observe that the proposed scheme perform much better in terms of accuracy as well as order of convergence for all α as compared to [69].

- **Numerical stability:** Figure 4.4 describes the numerical stability of our numerical scheme at different value of α. We have performed the simulation by adding a small disturbance (noise) δ=MAE, in the initial data at $M = 100$ and $N = 100$ grid points. It is observed that the variation in the MAE by adding noise, is almost negligible in comparison to the numerical results without noise. This verifies the stability of our numerical scheme.

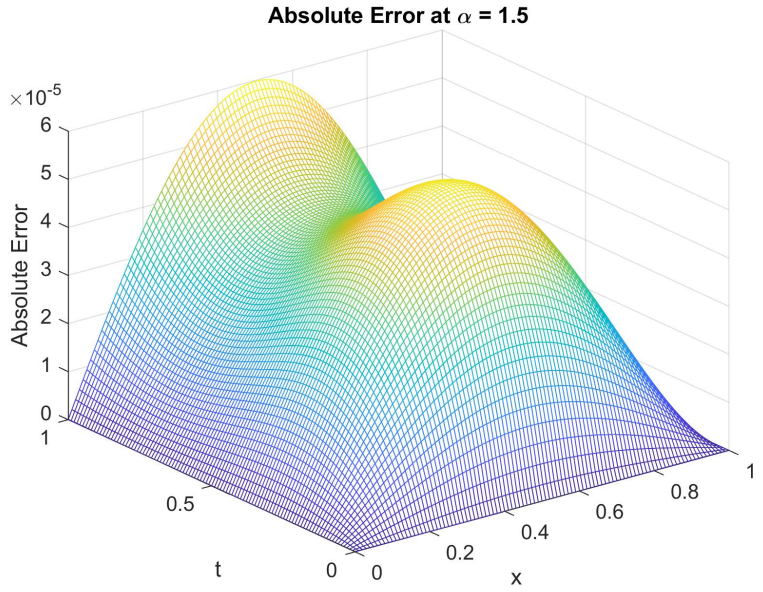

FIGURE 4.1: Surface plot of the absolute errors of Ex. 4.4.5 at $\alpha = 1.5$, $\tau = 1/100$, $h = 1/100$.

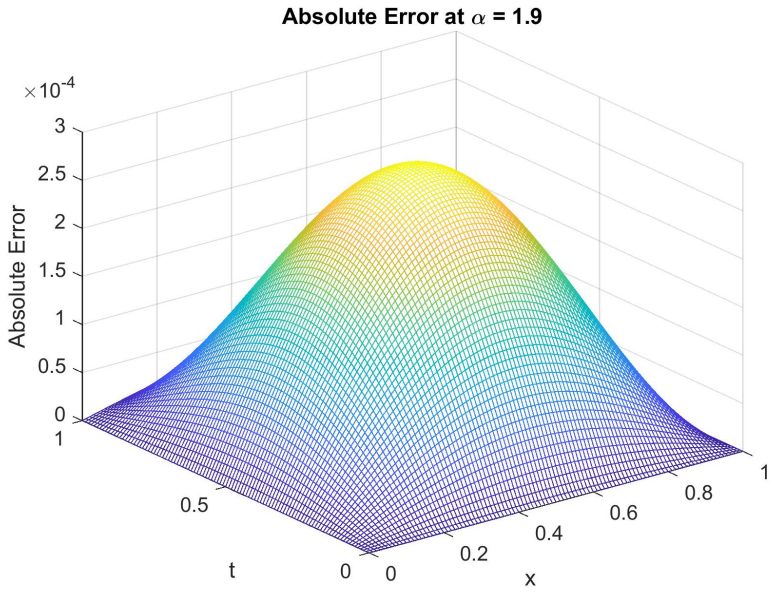

FIGURE 4.2: Surface plot of the absolute errors of Ex. 4.4.5 at $\alpha = 1.9$, $\tau = 1/100$, $h = 1/100$.

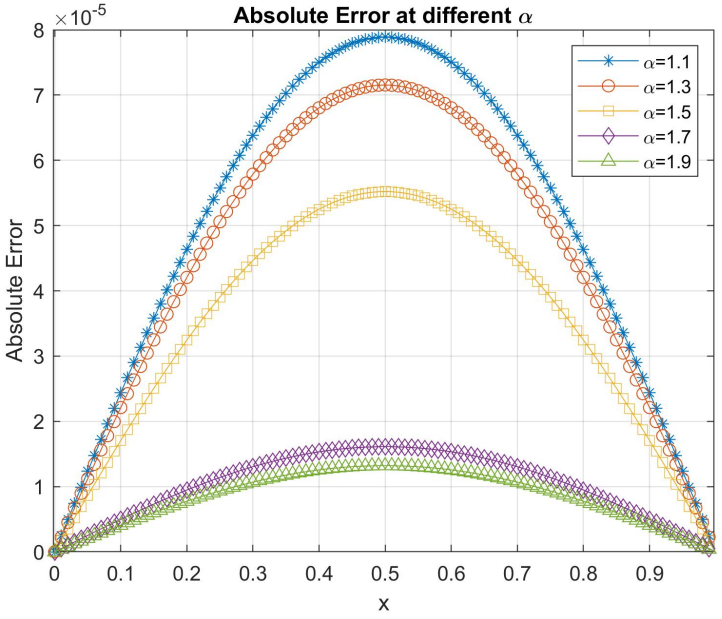

FIGURE 4.3: Absolute errors of Ex. 4.4.5 at time $T = 1$ for different α, $\tau = 1/100$, $h = 1/100$.

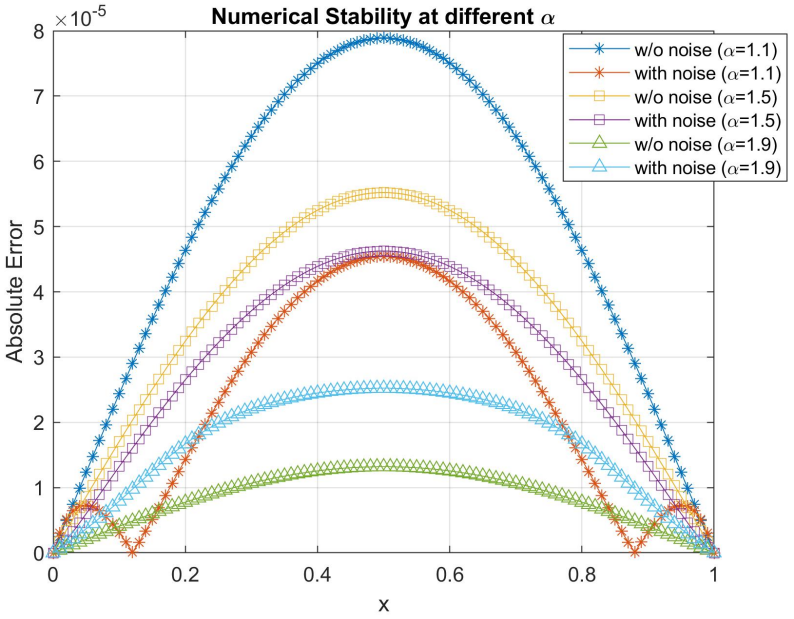

FIGURE 4.4: Numerical stability of Ex. 4.4.5 at $T = 1$ for different α, $\tau = 1/100$, $h = 1/100$.

τ	$\alpha = 1.1$		$\alpha = 1.5$		$\alpha = 1.9$	
	L_2 error	CO	L_2 error	CO	L_2 error	CO
1/40	8.319e-05	-	3.697e-05	-	8.102e-05	-
1/80	2.167e-05	1.940	1.033e-05	1.839	2.951e-05	1.457
1/160	5.595e-06	1.954	2.843e-06	1.862	8.053e-06	1.874
1/320	1.490e-06	1.909	8.130e-07	1.806	1.980e-06	2.024
1/640	4.533e-07	1.717	2.764e-07	1.557	4.334e-07	2.192

TABLE 4.5: L_2 error and order of convergence in Ex. 4.4.5 different values of α at time $T = 1$ when $h = 1/2000$.

τ	$\alpha = 1.1$		$\alpha = 1.5$		$\alpha = 1.9$	
	L_∞ error	CO	L_∞ error	CO	L_∞ error	CO
1/40	1.176e-04	-	5.228e-05	-	1.146e-04	-
1/80	3.065e-05	1.940	1.461e-05	1.839	4.174e-05	1.457
1/160	7.913e-06	1.954	4.020e-06	1.862	1.139e-05	1.874
1/320	2.107e-06	1.909	1.150e-06	1.806	2.800e-06	2.024
1/640	6.410e-07	1.717	3.909e-07	1.557	6.130e-07	2.192

TABLE 4.6: L_∞ error and order of convergence in Ex. 4.4.5 different values of α at time $T = 1$ when $\mathsf{h} = 1/2000$.

h	$\alpha = 1.1$		$\alpha = 1.5$		$\alpha = 1.9$	
	L_2 error	CO	L_2 error	CO	L_2 error	CO
1/5	1.711e-02	-	1.428e-02	-	1.018e-02	-
1/10	4.247e-03	2.011	3.559e-03	2.004	2.552e-03	1.996
1/20	1.060e-04	2.003	8.892e-04	2.001	6.384e-04	1.999
1/40	2.650e-04	2.000	2.223e-04	2.000	1.595e-04	2.001
1/80	6.634e-05	1.998	5.564e-05	1.999	3.972e-05	2.005
1/160	1.669e-06	1.991	1.397e-05	1.994	9.782e-06	2.022

TABLE 4.7: L_2 error and order of convergence in Ex. 4.4.5 different values of α at time $T = 1$ when $\tau = 1/1000$.

h	$\alpha = 1.1$		$\alpha = 1.5$		$\alpha = 1.9$	
	L_∞ error	CO	L_∞ error	CO	L_∞ error	CO
1/5	2.302e-02	-	1.920e-02	-	1.369e-02	-
1/10	6.006e-03	1.938	5.033e-03	1.932	3.609e-03	1.923
1/20	1.499e-03	2.003	1.258e-03	2.001	9.028e-04	1.999
1/40	3.747e-04	2.000	3.144e-04	2.000	2.255e-04	2.001
1/80	9.382e-05	1.998	7.868e-05	1.999	5.617e-05	2.005
1/160	2.360e-05	1.991	1.975e-05	1.994	1.383e-05	2.022

TABLE 4.8: L_∞ error and order of convergence in Ex. 4.4.5 for different values of α at time $T = 1$ when $\tau = 1/1000$.

α	τ	L_2 error		L_∞ error	
		L3 Scheme	Liu et al.[69]	L3 Scheme	Liu et al.[69]
1.1	1/5	3.333E-03	8.5162E-03	4.709E-03	1.2043E-02
	1/10	1.061E-03	2.2833E-03	1.500E-03	3.2290E-03
	1/20	3.082E-04	6.1932E-04	4.359E-04	8.7585E-04
	1/40	8.351E-05	1.6846E-04	1.181E-04	2.3823E-04
	1/80	2.199E-05	4.6015E-05	3.110E-05	6.5075E-05
	1/160	5.913E-06	1.2782E-05	8.362E-06	1.8077E-05
1.5	1/5	5.883E-03	3.1353E-02	8.319E-03	4.4340E-02
	1/10	6.076E-04	1.1325E-02	8.593E-04	1.6016E-02
	1/20	1.300E-04	3.9591E-03	1.838E-04	5.5990E-03
	1/40	3.723E-05	1.3859E-03	5.265E-05	1.9600E-03
	1/80	1.059E-05	4.8811E-04	4.146E-05	8.1965E-03
	1/160	3.109E-06	1.7260E-04	4.397E-06	2.4409E-04
1.9	1/5	2.671E-02	9.3759E-02	3.778E-02	1.3259E-01
	1/10	3.498E-03	4.9573E-02	4.946E-03	7.0107E-02
	1/20	6.752E-04	2.4983E-02	9.549E-04	3.5332E-02
	1/40	8.082E-05	1.2160E-02	1.143E-04	1.7197E-02
	1/80	2.932E-05	5.7958E-03	4.146E-05	8.1965E-03
	1/160	7.861E-06	2.7320E-03	1.117E-05	3.8637E-03

TABLE 4.9: Comparative study of L_2 error and L_∞ error for Ex. 4.4.5 at time $T = 1$ with $\mathsf{h} = 1/1000$ and different values of α.

Example 4.4.6. Consider the following TFWE with homogeneous boundary conditions

$$ {}_0^C\mathrm{D}_t^{\alpha}\mathfrak{U}(x,t) = \frac{\partial^2 \mathfrak{U}(x,t)}{\partial x^2} + \mathfrak{f}(x,t), \quad (x,t) \in [0,1] \times [0,1] \tag{4.64} $$

with initial and boundary conditions

$$\mathfrak{U}(x,0)=0,\ \mathfrak{U}_t(x,0)=0,\quad 0\le x\le 1, \tag{4.65}$$

$$\mathfrak{U}(0,t)=0,\ \mathfrak{U}(1,t)=0, \tag{4.66}$$

and source term is

$$f(x,t)=\frac{6t^{3-\alpha}}{\Gamma(4-\alpha)}x^{1+\alpha}(1-x)-t^3(\alpha+1)x^{\alpha-1}[\alpha-(2+\alpha)x]. \tag{4.67}$$

The exact solution of Ex. 4.4.6 is given by [69],

$$\mathfrak{U}(x,t)=t^3x^{1+\alpha}(1-x). \tag{4.68}$$

In this example, the absolute errors in Ex. 4.4.6, for $\alpha=1.5,\ 1.9$ and for different value of α are shown in Fig. 4.5, 4.6 and 4.7, respectively at $T=1$. The temporal and spatial order of convergence of the numerical scheme with respect to L_2 and L_∞ norm for different values of α are provided in Table 4.10-4.11 and Table 4.12-4.13 respectively. A comparison between L_2 and L_∞ error by the proposed scheme with the existing numerical results [69] are also given in Table 4.14 at $T=1$ when $h=1/1000$. This example also confirms that the proposed scheme gives high accuracy and convergence order as compared to [69]. Figure 4.8 verifies the numerical stability of our numerical scheme at different value of α. We have seen very small variation in the numerical result by adding a small noise in the initial data.

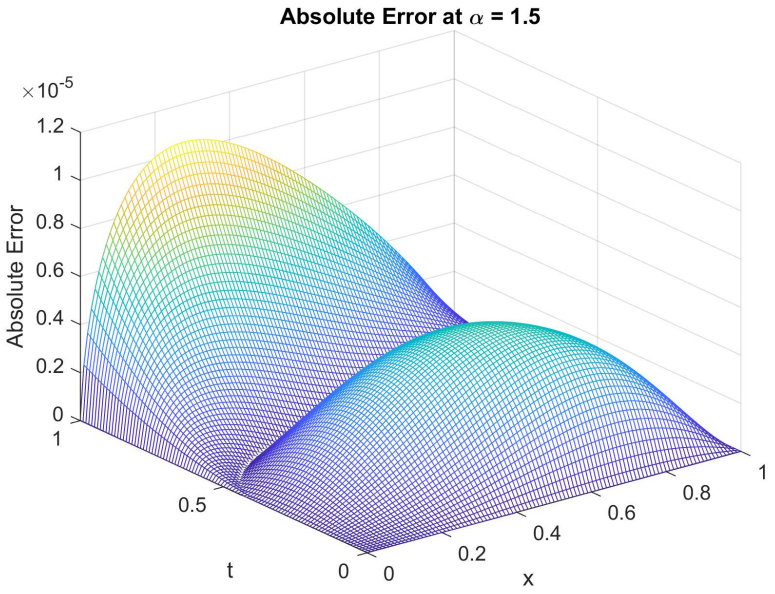

FIGURE 4.5: Surface plot of the absolute errors of Ex. 4.4.6 at $\alpha = 1.5$, $\tau = 1/100$, $h = 1/100$.

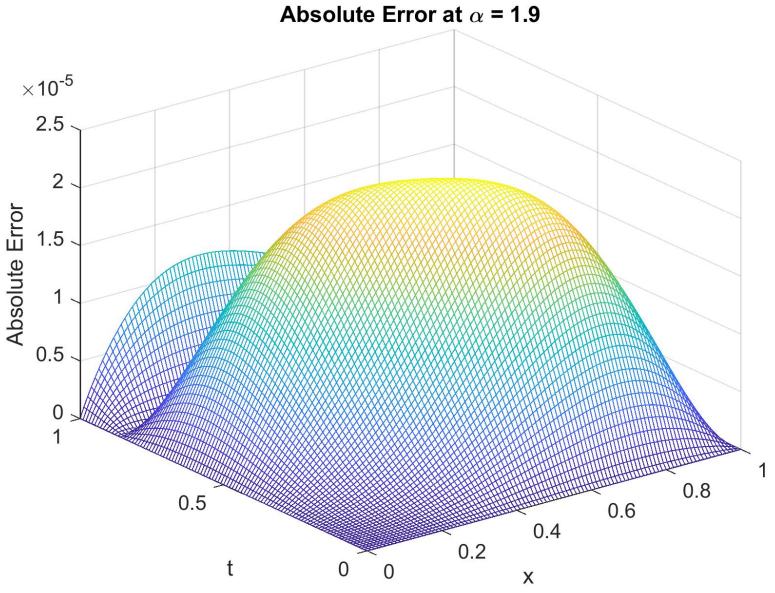

FIGURE 4.6: Surface plot of the absolute errors of Ex. 4.4.6 at $\alpha = 1.9$, $\tau = 1/100$, $h = 1/100$.

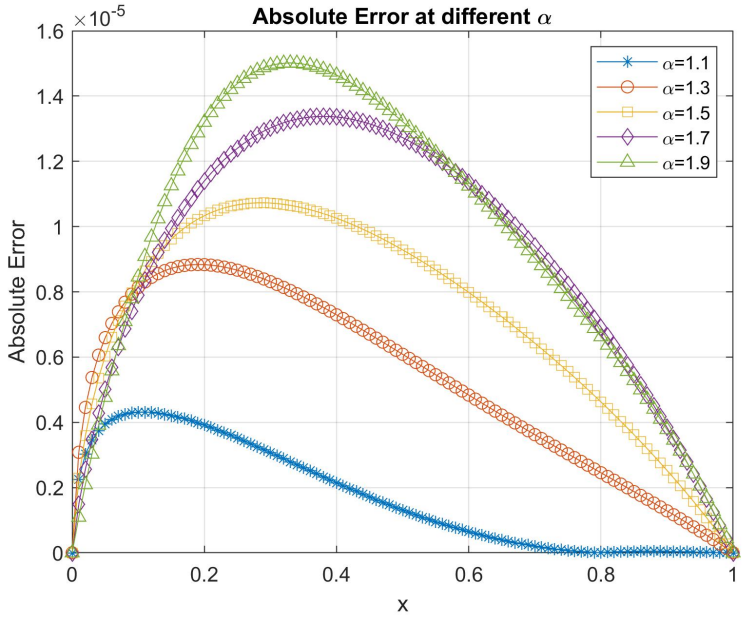

FIGURE 4.7: Absolute errors of Ex. 4.4.6 at time $T = 1$ for different α, $\tau = 1/100$, $h = 1/100$.

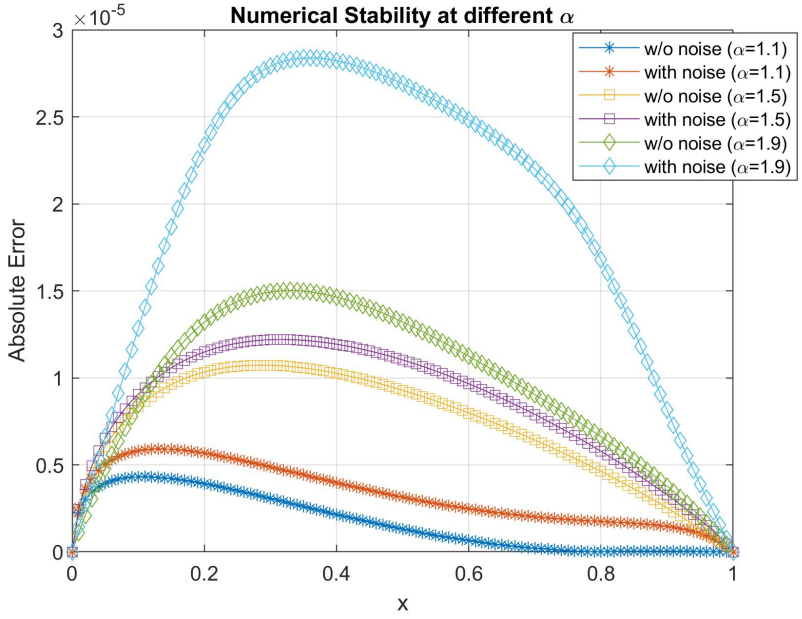

FIGURE 4.8: Numerical stability of Ex. 4.4.6 at $T = 1$ for different α, $\tau = 1/100$, $h = 1/100$.

τ	$\alpha = 1.1$		$\alpha = 1.5$		$\alpha = 1.9$	
	L_2 error	CO	L_2 error	CO	L_2 error	CO
1/40	1.011e-05	-	3.613e-06	-	8.740e-06	-
1/80	2.623e-06	1.946	9.940e-07	1.862	3.057e-06	1.516
1/160	6.648e-07	1.980	2.606e-07	1.931	8.295e-07	1.882
1/320	1.645e-07	2.015	6.239e-08	2.063	2.129e-07	1.962
1/640	3.823e-08	2.105	1.074e-08	2.538	5.721e-08	1.896

TABLE 4.10: L_2 error and order of convergence in Ex. 4.4.6 different values of α at time $T = 1$ when $\mathsf{h} = 1/3000$.

τ	$\alpha = 1.1$		$\alpha = 1.5$		$\alpha = 1.9$	
	L_∞ error	CO	L_∞ error	CO	L_∞ error	CO
1/40	1.439e-05	-	5.319e-06	-	1.572e-05	-
1/80	3.738e-06	1.944	1.456e-06	1.869	5.433e-05	1.532
1/160	9.489e-07	1.978	3.819e-07	1.930	1.469e-06	1.887
1/320	2.360e-07	2.007	9.300e-08	2.038	3.747e-07	1.971
1/640	5.596e-08	2.077	1.727e-08	2.429	9.868e-08	1.925

TABLE 4.11: L_2 error and order of convergence in Ex. 4.4.6 different values of α at time $T = 1$ when $\mathsf{h} = 1/3000$.

h	$\alpha = 1.1$		$\alpha = 1.5$		$\alpha = 1.9$	
	L_2 error	CO	L_2 error	CO	L_2 error	CO
1/5	2.935e-03	-	2.727e-03	-	2.935e-03	-
1/10	7.534e-04	1.962	7.384e-04	1.885	7.534e-04	1.962
1/20	1.899e-04	1.988	1.934e-04	1.933	1.899e-04	1.988
1/40	4.763e-05	1.995	4.980e-05	1.957	4.763e-05	1.995
1/80	1.193e-05	1.997	1.270e-05	1.972	1.193e-05	1.997
1/160	2.998e-06	1.993	3.214e-06	1.982	2.998e-06	1.993
1/320	7.619e-07	1.976	8.061e-07	1.995	7.619e-07	1.976

TABLE 4.12: L_2 error and order of convergence in Ex. 4.4.6 for different values of α at time $T = 1$ when $\tau = 1/1000$.

h	$\alpha = 1.1$		$\alpha = 1.5$		$\alpha = 1.9$	
	L_∞ error	CO	L_∞ error	CO	L_∞ error	CO
1/5	3.818e-03	-	3.667e-03	-	3.818e-03	-
1/10	9.794e-04	1.963	9.901e-04	1.889	9.794e-04	1.963
1/20	2.481e-04	1.981	2.596e-04	1.931	2.481e-04	1.981
1/40	6.221e-05	1.996	6.689e-05	1.957	6.221e-05	1.996
1/80	1.558e-05	1.997	1.705e-05	1.972	1.558e-05	1.997
1/160	3.916e-06	1.993	4.317e-06	1.982	3.916e-06	1.993
1/320	9.976e-07	1.973	1.085e-06	1.993	9.976e-07	1.973

TABLE 4.13: L_∞ error and order of convergence in Ex. 4.4.6 for different values of α at time $T = 1$ when $\tau = 1/1000$.

α	τ	L_2 error		L_∞ error	
		L3 scheme	Liu et. al.[69]	L3 scheme	Liu et. al.[69]
1.1	1/5	4.043E-04	1.0381E-03	5.726E-04	1.4799E-03
	1/10	1.288E-04	2.7833E-04	1.828E-04	3.9689E-04
	1/20	3.739E-05	7.5432E-05	5.314E-05	1.0758E-05
	1/40	1.007E-05	2.0454E-05	1.435E-05	2.9182E-05
	1/80	2.591E-06	5.5238E-06	3.704E-06	7.8901E-06
	1/160	6.337E-07	1.4716E-06	9.155E-07	2.1113E-06
1.5	1/5	5.647E-04	3.0298E-03	7.972E-04	4.3235E-03
	1/10	5.949E-05	1.0939E-03	8.796E-05	1.5597E-03
	1/20	1.277E-05	3.8251E-04	1.900E-05	5.4584E-04
	1/40	3.548E-06	1.3386E-04	5.244E-06	1.9114E-04
	1/80	9.288E-07	4.7079E-05	1.381E-06	6.7250E-05
	1/160	1.979E-07	1.6577E-05	3.081E-07	2.3694E-05
1.9	1/5	2.078E-03	7.2953E-03	3.013E-03	1.0400E-02
	1/10	2.905E-04	3.8455E-03	4.618E-04	5.4445E-03
	1/20	5.433E-05	1.9347E-03	8.322E-05	2.7264E-03
	1/40	8.793E-06	9.4082E-04	1.579E-05	1.3223E-03
	1/80	3.111E-06	4.4818E-04	5.511E-06	6.2913E-04
	1/160	8.854E-07	2.1117E-04	1.547E-06	2.9625E-04

TABLE 4.14: Comparative study of L_2 error and L_∞ error for Ex. 4.4.6 at time $T = 1$ with $\mathsf{h} = 1/1000$.

Example 4.4.7. Consider the following TFWE with homogeneous boundary conditions

$$ {}_0^C\mathrm{D}_t^\alpha \mathfrak{U}(x,t) = \frac{\partial^2 \mathfrak{U}(x,t)}{\partial x^2} + \mathfrak{f}(x,t), \quad (x,t) \in [0,\pi] \times [0,1] \tag{4.69} $$

with initial and boundary conditions

$$\mathfrak{U}(x,0) = 0,\ \mathfrak{U}_t(x,0) = 0, \quad 0 \le x \le \pi, \tag{4.70}$$

$$\mathfrak{U}(0,t) = 0,\ \mathfrak{U}(\pi,t) = 0, \tag{4.71}$$

and source term

$$f(x,t) = \left(\frac{\Gamma(3+\alpha)}{2} + t^{\alpha}\right) t^2 \sin(x). \tag{4.72}$$

The exact solution of Ex. 4.4.7 is given by [111],

$$\mathfrak{U}(x,t) = t^{2+\alpha} \sin(x). \tag{4.73}$$

The following points from Ex. 4.4.7 are:

- Fig. 4.9 and 4.10 shows absolute errors in Ex. 4.4.7, for $\alpha = 1.5$ and $\alpha = 1.9$ respectively, when $\tau = 1/100$ and $h = 1/100$.
- Table 4.13 gives the L_2 error, MAE and the order of convergence in temporal direction for different values of alpha at $T = 1$, when $h = \pi/5000$.
- A comparative study of the numerical results with the existing results [111] in Table 4.13 and 4.15 shows that the proposed algorithm provides almost the same accuracy.
- Table 4.14-4.15 demonstrates the L_2 error, MAE and the order of convergence in spatial direction for different values of alpha, when $\tau = 1/2000$.
- Figure 4.12 describes the numerical stability of our numerical scheme at different value of α.

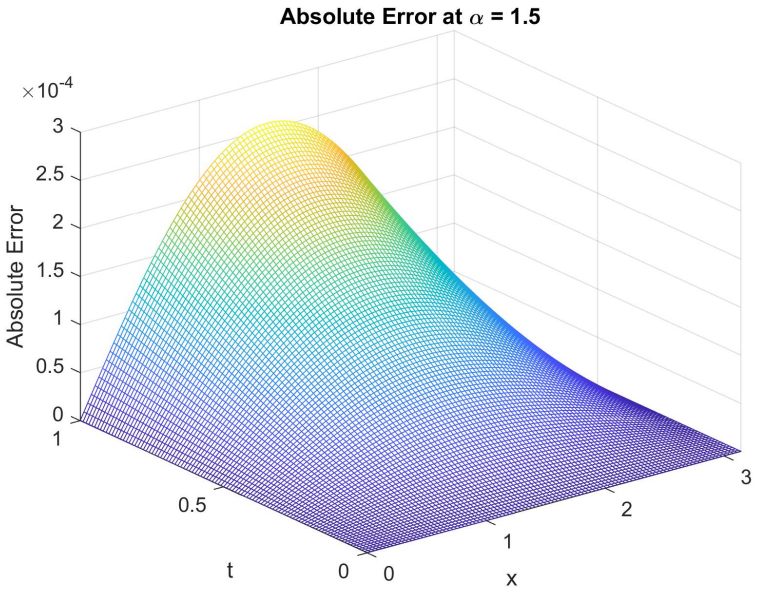

FIGURE 4.9: Surface plot of the absolute errors of Ex. 4.4.7 at $\alpha = 1.5$, $\tau = 1/100$, $h = 1/100$.

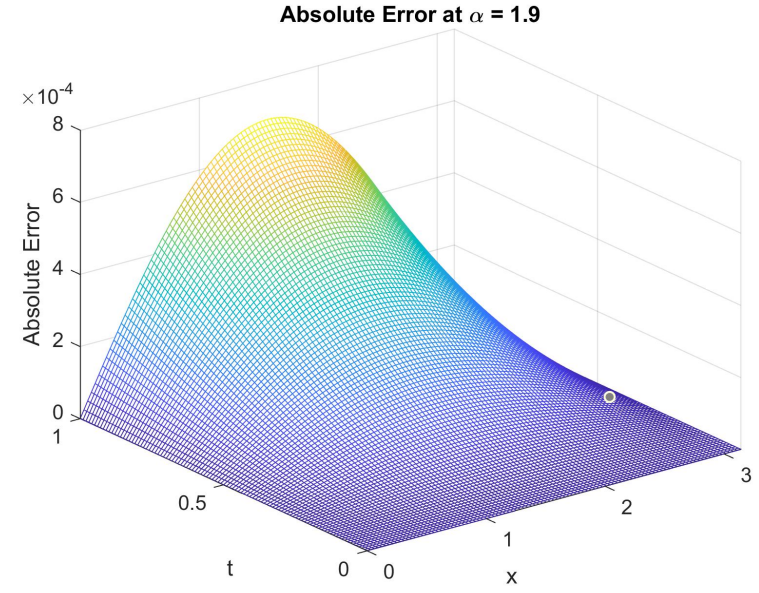

FIGURE 4.10: Surface plot of the absolute errors of Ex. 4.4.7 at $\alpha = 1.9$, $\tau = 1/100$, $h = 1/100$.

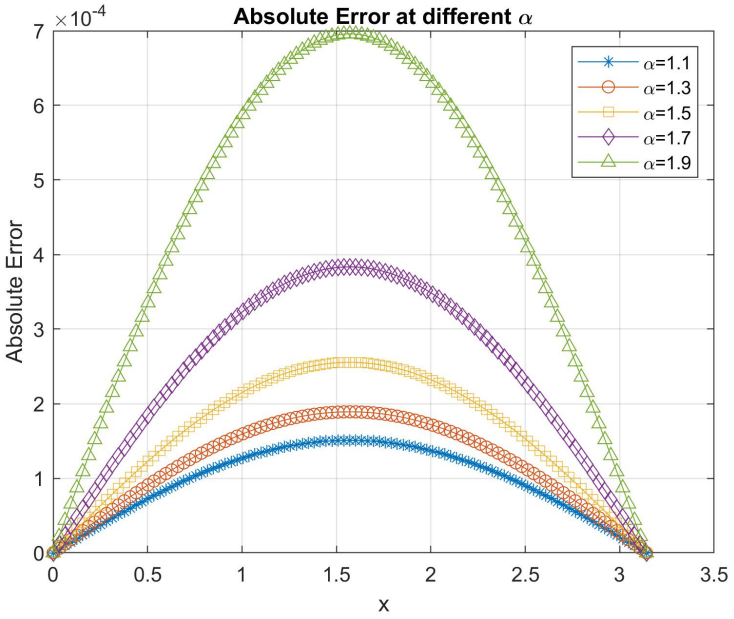

FIGURE 4.11: Absolute errors of Ex. 4.4.7 at time $T = 1$ for different α, $\tau = 1/100$, $\mathsf{h} = 1/100$.

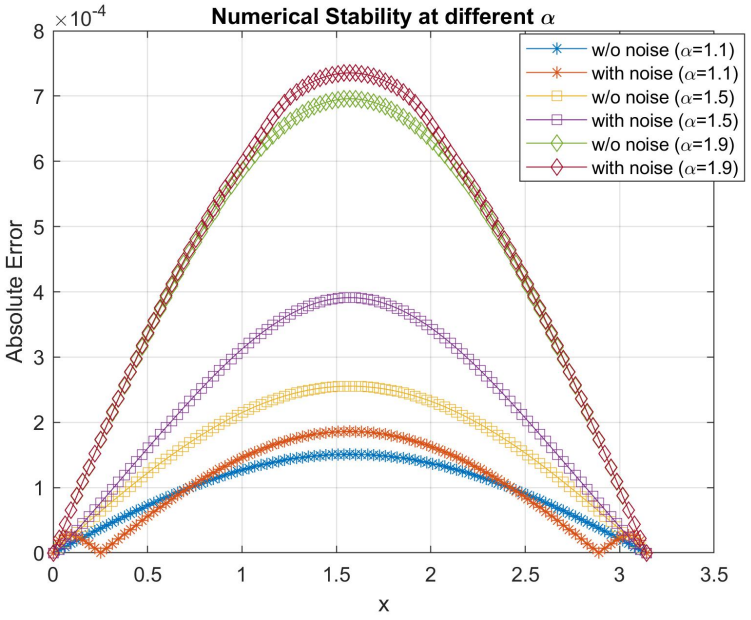

FIGURE 4.12: Numerical stability of Ex. 4.4.7 at $T = 1$ for different α, $\tau = 1/100$, $h = 1/100$.

α	τ	L3 Scheme				Sun et. al.[111]	
		L_2 error	CO	MAE	CO	MAE	CO
1.1	1/80	2.719e-04		2.169e-04	-	1.9809e-04	-
	1/160	6.814e-05	1.996	5.437e-05	1.996	4.9875e-05	1.990
	1/320	1.708e-05	1.996	1.363e-05	1.996	1.2548e-05	1.992
1.5	1/80	4.917e-04		3.923e-04	-	1.9396e-04	-
	1/160	1.204e-04	2.030	9.608e-05	2.030	4.9309e-05	1.976
	1/320	2.967e-05	2.021	2.367e-05	2.021	1.2471e-05	1.984
1.9	1/80	1.355e-03		1.018e-03	-	5.6352e-05	-
	1/160	3.288e-04	2.043	2.624e-04	2.043	1.4511e-05	1.957
	1/320	7.966e-05	2.045	3.356e-05	2.045	3.6866e-06	1.978

TABLE 4.15: L_2 error, Maximum absolute error (MAE) and order of convergence in Ex. 4.4.7 for different values of α at time $T = 1$ when $h = \pi/5000$.

h	$\alpha = 1.1$		$\alpha = 1.5$		$\alpha = 1.9$	
	L_2 error	CO	L_2 error	CO	L_2 error	CO
$\pi/5$	7.333e-03	-	3.711e-03	-	1.658e-03	-
$\pi/10$	1.845e-03	1.991	9.361e-04	1.987	4.197e-04	1.982
$\pi/20$	4.624e-04	1.997	2.351e-04	1.994	1.066e-04	1.977
$\pi/40$	1.160e-04	1.995	5.936e-05	1.986	2.807e-05	1.925
$\pi/80$	2.932e-05	1.984	1.540e-05	1.947	8.429e-06	1.736

TABLE 4.16: L_2 error and order of convergence in Ex. 4.4.7 for different values of α at time $T = 1$ when $\tau = 1/2000$.

h	$\alpha = 1.1$				$\alpha = 1.5$		$\alpha = 1.9$	
	L_∞ error	CO	L_∞ error	[111]	L_∞ error	CO	L_∞ error	CO
$\pi/5$	5.565e-03	-	-	-	2.816e-03	-	1.258e-03	-
$\pi/10$	1.472e-03	1.918	1.4722e-03	-	7.469e-04	1.915	3.349e-04	1.909
$\pi/20$	3.689e-04	1.997	3.6887e-04	1.997	1.876e-04	1.994	8.504e-05	1.977
$\pi/40$	9.253e-05	1.995	9.2496e-05	1.996	4.736e-05	1.986	2.240e-05	1.925
$\pi/80$	2.340e-05	1.984	-	-	1.229e-05	1.947	6.725e-06	1.736

TABLE 4.17: L_∞ error and order of convergence in Ex. 4.4.7 for different values of α at time $T = 1$ when $\tau = 1/2000$.

4.5 Conclusion

In summary, we have proposed two novel approximation called L3 and modified L3 approximation (ML3) for the Caputo derivative of order $\alpha \in (1, 2)$. Both the approximations are observed to be highly accurate and of second order. We have applied L3 approximation to develop a difference scheme to solve TFWE. Both the approximations are tested on four numerical examples, and the numerical scheme with L3 approximation is verified on three problems of TFWEs. The numerical results are highly accurate. The comparative study of the numerical results with the existing results is also provided in Table 4.9, 4.14, 4.15, and 4.17. It is concluded that the proposed numerical scheme is simple, highly accurate and can be acceptable to solve TFPDE when $\alpha \in (1, 2)$.

4.5.1 Future work

Now we proposed some future works for the readers which is based on the scheme presented in this chapter:

- To discuss the theoretical stability and convergence of the proposed numerical scheme.
- To extend the L3 and ML3 approximation on more complex boundary conditions.
- To develop the L3 and ML3 approximation on non-uniform mesh.
- To develop a numerical scheme for the non-linear problem in higher dimension.
- The validate the proposed scheme for non-smooth solution.

****